CRONOBACTER SAKAZAKII CHARACTERIZATION AND ANALYSIS OF CYTOTOXICITY IN MICROVASCULAR ENDOTHELIAL CELLS

A Thesis
Submitted to the Graduate Faculty
of the
North Dakota State University
of Agriculture and Applied Science

By

Hilary Jayne Hafner

In Partial Fulfillment
for the Degree of
MASTER OF SCIENCE

Major Department:
Microbiology

March 2014

Fargo, North Dakota

North Dakota State University
Graduate School

Title

CRONOBACTER SAKAZAKII CHARACTERIZATION AND ANALYSIS OF CYTOTOXICITY IN MICROVASCULAR ENDOTHELIAL CELLS

By

Hilary Jayne Hafner

The Supervisory Committee certifies that this ***disquisition*** complies with North Dakota State University's regulations and meets the accepted standards for the degree of

MASTER OF SCIENCE

SUPERVISORY COMMITTEE:

Birgit Pruess
Chair

Penelope Gibbs

Nathan Fisher

David Wells

Approved:

March 28, 2014	Charlene Wolf-Hall
Date	Department Chair

ABSTRACT

Contamination of powdered infant formulas by the bacteria *Cronobacter sakazakii* can pose serious risk to infants and neonates who consume the formula and subsequently develop *C. sakazakii* related illnesses such as sepsis and meningitis (1).

The Gibbs' lab assesses *C. sakazakii* isolates' ability to cross the blood brain barrier and cause meningitis. This thesis research investigated *C. sakazakkii* cytotoxicity towards microvascular endothelial cells which comprise the first cell line encountered in the barrier. Understanding the mechanisms used to affect these cells will contribute to our understanding of early stages of invasion.

Cytotoxicity assays performed for this research found that the cell line used could not sustain confluency when co-cultured with *C. sakazakii* isolates over periods beyond 24 hours of incubation. In addition, cell-free cytotoxicity assays found that live cells are not necessary to cause damage suggesting a toxin mediated effect.

ACKNOWLEDGEMENTS

I'd like to sincerely thank both Dr. Pruess and Dr. Gibbs for agreeing to help me work on a joint project between the two labs. I appreciate the guidance and support from both of you and could not have asked for better advisors. I've gained a great deal of confidence and independence from your leadership and faith in me. I'd like to thank all my labmates in both labs for their insights and support. Working in a positive environment has made my research even more enjoyable.

Shelley Horne and Heather Vinson were both instrumental to helping me design and carry out my research assays and experiments. Their patience, guidance, and suggestions in the lab have helped shape my approach and attention to detail when performing lab work. Thank you both for your time and the phenomenal amount of help you have given me.

Scott Hoselton and Pawel Borowicz are my microscope heroes. Thank you so much for taking time out to explain to me how the microscopes in your respective labs work and for teaching me how to optimally use them. A large portion of my data consists of images illustrating cell damage. These images would not be of thesis quality without your help! I'd also like to thank Scott for recommending staining techniques and reagents to help better visualize my cells-your advice was much needed.

Elliott Welker's prior work with *C. sakazakii* and the TEER model shaped my understanding of my own research and experiments. Thank you, Elliott for steering me in the right direction and sharing your insights.

I'd also like to thank all of my past and present committee members: Dr. Haring, Dr. Fisher, and Dr. Wells. Thank you for your time and input. I really appreciate all the advice and

direction I’ve received. Your thoughtful questions and inquiries have pushed me to think about the big picture view of my research and enhanced my drive to be a better research scientist.

Last but not least, I’d like to thank my husband Nick for his patience with midnight time points, his willingness to sacrifice weeknights/weekends/holidays with me during experiments and thesis writing, and most of all for his unfaltering support of me when I needed it most. Your constant love and encouragement means the world to me. SFTMLS.

TABLE OF CONTENTS

LIST OF TABLES

Table Page

LIST OF FIGURES

Figure Page

LITERATURE REVIEW

Research Note & History of the *Cronobacter* Genus

The research done for this thesis focuses on the species *Cronobacter sakazakii.* This species is not synonymous with *Enterobacter sakazakii*. The old *E. sakazakii* designation refers to what is today recognized as multiple *Cronobacter* species including *C. sakazakii* and nine others. Much of the early research pertaining to general characteristics of *Cronobacter* was done under the *E. sakazakii* designation and is therefore still pertinent to this study. Any literature prior to 2007 referring to *E. sakazakii* will be noted as: *Cronobacter Complex* throughout the thesis to make a clear distinction between references to multiple and single species.

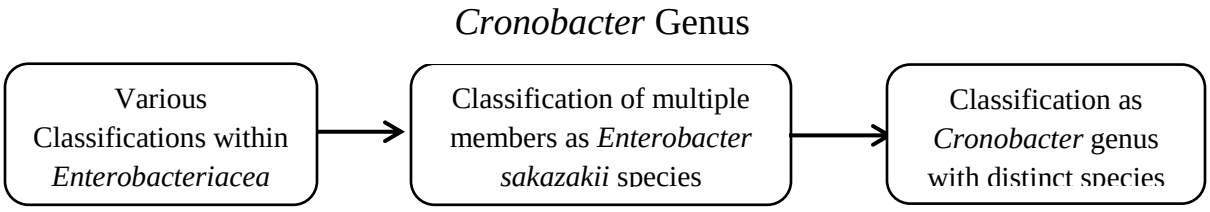

Figure 1: *Cronobacter* Genus Naming History

The *Cronobacter* genus has a complex history that began in 1980 and continues today as advances in technology have made clear classification within the genus possible (2–7). Initially, species of the *Cronobacter* genus were not recognized distinctly from other species within the *Enterobacteriaceae* family and were classified with various names such as "yellow pigmented *Enterobacter cloaceae*" (3). The first reclassification began with multiple members of the *Cronobacter* genus being grouped together as one species in the *Enterobacter* genus as *E. sakazakii* (3, 4). As more sophisticated genetic analysis became available, the *E. sakazakii*

species was recognized as several distinct species and the *Cronobacter* genus was created (4). New species continue to be classified into the genus as taxonomic resolutions and discoveries continue to be made (6, 7).

Classification into *Enterobacter sakazakii* Species

Prior to 1980, members of the *Cronobacter* genus were classified under various names including: "yellow pigmented *E. cloaceae*", "yellow coliform", *Serratia sp.,* and *Chromobacterium* (3). In 1980 Farmer et al. proposed that the organism formerly classified as "yellow pigmented *Enterobacter cloacae*" be separated into a separate species,"*E. sakazakii,*"; this was done based on DNA-DNA hybridization experiments which showed that the organism met criteria to form its own species (3).

Classification of the *Cronobacter* Genus

In 2007, further taxonomic studies provided data to support placing *E. sakazakii* into a novel genus, *Cronobacter,* and to separate the genus into five species and one genomospecies: *C. sakazakii, C. malonaticus, C. turicensis, C. muytjensii, C. dublinensis,* and *C.* genomospecies 1(4). The genomospecies was later classified in 2011 as *C. universalis* and at this time *C. condiment* was shown to be a novel species as well (7). As of the fall of 2013, an additional 3 species (*C. zurichensis, C. helveticus, and C. pulveris*) were identified and added to the *Cronobacter* genus bringing the total number of species up to 10 (6, 8). These three species were originally classified between 2007-2008 as *Enterobacter* species, but were recently re-classified into the *Cronobacter* genus with their original species designations (except for *E. turicensis)* after further genetic analysis(6, 9, 10).

Etymology of the *Cronobacter* Genus Nomenclature

The original designation of *E. sakazakii* was proposed in honor of Riichi Sakazakii, a Japanese microbiologis, veterinarian, and taxonomist who contributed substantially to the study of *Enterobacteriaceae* and named several species in the genus (3, 11).

When research warranted the addition of a novel genus for *Enterobacter sakazakii*, *Cronobacter* was chosen to represent the Greek Titan Cronus who consumed his children at birth to prevent them from overthrowing his rule(12, 13). Cronus was chosen due to the notoriety of the species *C. sakazakii* and its ability to cause rare but often fatal cases of neonatal meningitis which causes swelling of the tissues surrounding the infant brain (4, 14).

The first five species identified in the genus were named according to their original country of discovery, after notable researchers, or due to their unique biochemical properties or (4). The first species contained the largest number of isolates and was named *C. sakazakii* to continue to honor the work of Riichi Sakazakii; the type strain for this organism remains ATCC 29544 which was originally obtained from a throat culture taken from a patient in Tennessee in 1970 and designated by the CDC as 4562-70 (3, 4). *C. malonaticus* was originally proposed as a subspecies of *C. sakazakii* but later was shown to be a closely related but distinct species; it was named for the use of malonate which varies within the genus (4, 15). *C. muytjensii* was named to honor another microbiologist, Henry Muytens, who contributed to the initial studies of *Enterobacter sakazki;* the type strain for this species is ATCC 51329 (4). Both *C. dublinensis and C. turicensis* were named for the cities that the proposed type strains originated from: Dublin, Ireland and Zurich, Switzerland respectively(4).

The five speices that were added to the *Cronobacter* genus after 2007 were named as follows. *C. condiment* was isolated from a spiced meat product and references the origin of the organism in condiments; *C. unversalis* was proposed as a distinct species designation for strains previously designated in the genomospecies 1 group (7). Both *C. zurichensis* and *C. helveticus* were named for their origins in Zurich and Helvetica Switzerland; *E. turcensis* was renamed as *C. zurichensis* as the name was already used in the *Cronobacter* genus to designate another distinct species(6). *E. pulvaris* was reclassified as *Cronobacter* under the same species name which originated from its discovery as a contaminant in powdered products (6, 9).

General Characteristics of *Cronobacter Complex* and *C. sakazakii*

The *Cronobacter* genus belongs to the class *Gammaproteeobacteria* and the family *Enterobacteriaceae* (7). It contains Gram negative rods that measure 3 microns by 1 micron, and are facultative anaerobes that are generally motile by peritrichous flagella; they do not form spores (3, 4). One gene contained in all sequenced members of this family is the *crtZ* gene which codes for the characteristic yellow pigment; however not all *Cronobacter* species express the gene (5, 16). Characteristic biochemical test results are extensively described by both Farmer et al and Iverson et al (3, 4). Studies have reported that members of this genus can grow at temperature ranges between 6 ^{o}C and 47 ^{o}C, with an optimal growing range between 37 ^{o}C and 43 ^{o}C (2, 17, 18). At an optimal growing temperature of 37 ^{o}C, *Cronobacter Complex* double on average every 22 minutes (17). The growth characteristics of the species is dependent upon growth conditions, environmental stress, and media used; studies have shown that these bacteria do not grow the same in food products as they do in laboratory simulated conditions meant to mimic them (19–21).

C. sakazakii and *Cronobacter Complex* can be found ubiquitously in the environment on various locations including: solid and liquid food products, households, factory settings, and even within insects such as flies (22–25). Plants have been suggested as the natural reservoir for the organism (26). A review of literature pertaining to globally contaminated food products showed *Cronobacter Complex* can be found on cereal products, legumes, tea/spices, fruits, vegetables, dairy products, meat products and even in water sources (22). Notably, *Cronobacter Complex* has been found to contaminate powdered infant formula (PIF) in 13 different countries, including: Australia, Canada, France, Germany, India, and the US (24). Contaminated PIF has been associated with serious neonatal diseases which will be discussed under 'Clinical Significance' (27–32).

The survival traits associated with *C. sakazakii* and *Cronobacter Complex* have been attributed to the organism's ability to persist in such varied environmental locations, including food products (19, 18, 33, 17, 34). Of note is the organism(s)' ability to survive drying, osmotic, and heat stress (18, 33, 34). Studies of *Cronobacter Complex* have shown that some isolates can survive for up to 2.5 years in dehydrated powdered infant formula which can be an important food contamination vehicle and that in general, these organisms can survive drying better than other members in the *Enterobacteriaceae* family such as *E. coli* (18, 33). The ability of this group to survive heat stress was initially debated as studies showed conflicting results with respect to thermal tolerance (18, 34). Later studies showed that heat tolerance is dependent on the strain of *Cronobacter Complex* and the growth conditions used (20). Certain isolates have been shown to survive temperatures as high as 58-60 ^{o}C with stationary cells at near-neutral pH (20, 21, 34). Nine thermotolerant strains of *C. sakazakii* surviving for 102- 217 s at 58 C have been reported and were found to share the same DNA marker for heat resistance,. *orf*I (35, 36).

Heat stress has also been shown to affect the antibiotic resistance of *C. sakazakii* which results in increased resistance to a number of antibiotics including gentamicin and ampicillin which are used for treatment in *C. sakazakii* associated meningitis (19).

Antimicrobial Susceptibility Characteristics

Cronobacter Complex was initially reported by Farmer et al to be sensitive to the protein synthesis inhibiting antibiotics gentamicin, kanamycin, and the cell wall inhibiting antibiotics ampicillin and chloramphenicol (3). Clinical reviews agree with these findings and report that in addition, these bacteria are also sensitive to penicillin and third generation cephalosporins and the antimetabolite trimethroprim sulfamethazide although at least five cases have shown resistance to ampicillin (32). *Cronobacter Complex* show resistance to beta-lactams (32, 37).

In a study of different strains of *C. sakazakii*, unstressed bacteria were sensitive to: the protein inhibiting aminoglycosides streptomycin, gentamicin, and kanamycin; the cell wall disrupting penicillin amoxicillin;and to the nucleic acid disrupting flouroquinolone ciprofloxacin (19). These same strains were resistant to the aminoglycoside neomycine, to two protein inhibiting tetracyclines-tetracycline and doxycycline- and the cell wall synthesis inhibiting antibacterial drug vancomycin (19).

Clinical Significance

Cronobacter Complex and *Cronobacter sakazakii* are able to cause disease across age groups, but have the most severe impact on the immune-compromised portion of the population including neonates and the elderly (1, 32). Due to the re-classification of *Cronobacter Complex*in 1980 and *C. sakazakii* in 2007, it is at times difficult to track historical cases of disease and to

distinguish which species is the causative agent of disease without retrospective investigation (2, 28).

Diseases associated with *Cronobacter Complex* include: bacteremia, conjunctivitis, dermoid cysts, diarrhea, neonatal meningitis, necrotizing enterocolitis (NEC), sepsis, urinary tract infections, and wound infections (1, 27–32, 38). These diseases most often affect infants and neonates (1, 27–32, 38).

The current surveillance systems in place do not actively monitor infections caused by *C. sakazakii* or other *Cronobacter* species although Minnesota enacted mandatory passive surveillance for invasive infection in children in 2005 (1, 28). Therefore, due to lack of active reporting and small existing data sets, the incidence and disease prevalence caused by *Cronobacter sakazakii* and other *Cronobacter* species have not been established (28).

In a global call for data, the Food and Agricultural Organization of the United Nations (FAO) and World Health Organization (WHO) found that reported infections caused by *Cronobacter* species in neonates and infants often progress to NEC, meningitis, and bacteremia (28). The mechanism of pathogenesis leading to these diseases remains unknown although researches have begun to elucidate several virulence related characteristics and genes (39–41).

Meningitis Symptoms, Treatment, and Outcomes in Infants

Meningitis is characterized by an inflammation of the membranes that surround and protect the brain (14). The Centers for Disease Control and Prevention describe the symptoms of infant and neonatal meningitis as nonspecific and may "include [. . . fever], poor feeding, and listnessness (1)." The CDC reports that diagnosis is usually made through laboratory testing and culture of blood and or cerebrospinal fluid followed by appropriate identification steps (42). The

outcomes of *Cronobacter Complex* associated meningitis can range from complete recovery to severe complications such as quadriplegia, brain cysts, developmental delays, mental retardation, and death (28, 30, 32, 38).

Cronobacter species that have been associated with meningitis are : *C. sakazakii, C. malonaticus,* and *C. turicensis* (4). Current treatment for meningitis associated with these species includes the use of third generation cephalosporin in conjunction with gentamicin and ampicillin (32). Meningitis-related fatality rates associated with *Cronobacter* species vary by individual outbreak; however, of the known cases reviewed by the FAO and WHO the overall fatality rate is 40% with some survivors experiencing severely impaired brain function (27, 28, 32).

Pathogenesis

Virulence traits and pathogenic mechanisms associated with *C. sakazakii* and other species within the genus remains largely unknown, although initial studies have begun the process of identifying specific genes, properties, and pathways involved in the infection process.

Initial research on *C. sakazakii* and *Cronobacter Complex* has revealed that these species are able to form biofilms, possess iron acquisition genes, and are able to persist in human macrophages (8, 16, 37, 43–45). *Cronobacter Complex*also possess zinc metalloproteases which can target host cells (16, 46). One *C. sakazakii* plasmid, pESA3, codes for a plasminogen activator and Type Six Secretion System (highly variant) which are associated with resistance to complement activity and molecular delivery respectively (41, 44). The endotoxin of *Cronobacter Complex* has been shown to increase the bacterial ability to translocate cells in rat intestines, although other secreted factors are suspected to aid in translocation (47). Such factors could be

delivered through an intact Type Six Secretion System which some *Cronobacter* Complex species possess (16).

Tissue culture studies have shown that specific isolates of *C. sakazakii* and *Cronobacter Complex* are able to adhere to and invade a number of cell lines including the following human cell types: Caco-2 intestinal epithelial cells, INT 407 intestinal epithelial cells, brain microvascular endothelial cells, brain capillary endothelial cells and can survive within macrophages (39, 40, 45, 48–50). Adherence occurs in either aggregate or diffuse patterns and invasion rates of specific cell lines vary between isolates ranging from high to low (39, 51). Disruption of host cell tight junctions has been shown to increase invasion rates of the above mentioned intestinal epithelial cell lines and is suspected to increase invasion in endothelial cells as well (40, 45).Outer membrane proteins OmpA and OmpX are required for invasion of Caco-2 and INT 407 cell lines while invasion of brain microvascular endothelial cells requires cytoskeleton rearrangement through the utilization of host P13K/Akt signaling pathway (40, 49, 50).

Blood Brain Barrier

The blood brain barrier (BBB) is composed of three major cell that are responsible for forming a selectively permeable barrier which ensures the brain maintains homeostasis (52–54). These cell types include brain microvascular endothelial cells (BMEC), glial cells called astrocytes, and pericytes which are related to smooth muscle cells (14, 52–54). Together, the astrocytes and pericytes help maintain barrier properties while providing structural support (52, 53).

The tight junctions between BMECs of the blood brain barrier differ from junctions elsewhere in terms of their complexity and tightness between cells (52, 55). BBB tight junctions are 50-100x tighter than other junctional complexes and provide high electrical resistance that helps restrict paracellular movement and prevent the free diffusion of harmful solutes (52, 55). The lipid membranes of the BBB cells allow free movement of oxygen, carbon dioxide, ethanol and fat soluble molecules through the plasma while other essential nutrients must use carrier systems to cross the barrier; harmful substances and non-essential nutrients cannot access the barrier and are actively removed (14, 52).

C. sakazakii Traversal of BBB

Pathogenic invasion of the blood brain barrier is incompletely understood and most likely involves complex host-pathogen interactions (56, 57). Disease progression from *C. sakazakii* infection in neonates has been linked with contaminated powdered infant formula and is proposed to progress from NEC cases. In a review of bacterial meningitis, the progression is proposed to occur as follows: invasion of and escape from the gut followed by survival in the blood until contact and invasion of the blood brain barrier is achieved (58). In *C. sakazakii*, meningitis could develop after NEC infection by the same route. After ingestion of contaminated PIF, the bacteria must colonize the gut epithelium. To cause initial infection; the bacteria must also invade these cells and develop into necrotizing enterocolitis, then bacteremia (59). As previously stated, *Cronobacter* complex has been shown to be able to invade intestinal epithelial cells *in vitro* (39, 48). Once in the blood, *C. sakazakii* must maintain high numbers and travel to sites of the blood brain barrier where it must finally cross the barrier to cause meningitis (60).

Survival in the blood may be possible in part due to *Cronobacter* plasminogen activator which confers resistance to components of the innate immunes system such as C3, C3a, and C4b (41).

Bacterial traversal of the blood brain barrier is proposed to occur via three possible mechanisms: paracellular, transcellular, or by phagocytic transport (54, 60). Among meningitis causing pathogens, more than one method of traversal may be utilized by the same organism (53, 54). Two possible mechanisms appear possible for *C. sakazakii:* transcellular and phagocytic transport. Studies have shown that *C. sakazakii* can survive within macrophages which are able to cross the BBB (45). In addition, one type of neuroglia cell of the BBB, microglial cells, can differentiate into macrophages when bacteria are present (14). Phagocytized bacteria could survive traversal within either circulating or differentiated macrophages. Transcellular traversal investigation has shown that *C. sakazakii* is able to invade brain microvascular endothelial cells and to cause cytoskeletal rearrangements via P13K/Akt signal transduction (39, 45, 49, 50).

Research Experiments and Rationale

Our research with *C. sakazakii* aims to enhance both our understanding of the transcellular mode of traversal as well as bacterial BBB traversal as a whole. *C. sakazakii* isolates from clinical cases and fecal sources were studied to detect the cytotoxic effects of the species on mouse endothelial cells and to assess the suitability of the endothelial cell line for use in an astrocyte-endothelial co-culture system which is currently under development in Dr. Gibbs lab. The use of such a system will contribute to our overall understanding of bacterial interaction with the BBB as various pathogens could be inoculated into the system and observed.

Isolates were first characterized with respect to growth, antibiotic susceptibility, and motility to compare individual isolate characteristics to existing literature. The isolates used

show growth and antibiotic susceptibility patterns that are similar to those described previously (17, 61).

Next, isolates were cultured with endothelial cells to assess cytotoxicity over long-term incubation periods both with whole cell samples and cell-free supernatant. All whole-cell isolates damage the endothelial cells after 24 hours, causing cell rounding and death. The most cytotoxic isolate, BAA 894 was chosen for further study with cell-free supernatant. This isolate caused similar damage to EOMA cells as the whole-cell sample, although damage occurred earlier. These findings show that live bacteria are not required for cell damage and that the effects seen may be a result of a combination of contact and toxin mediated damage.

Invasion and adhesion assays were also performed to assess whether the *C. sakazakii* isolates are able to invade the mouse endothelial cells similar to invasion seen in human endothelial cell lines. This would ensure that the use of the mouse system closely mimics true pathology in human cells. The invasion and adhesion assays were not completed due to time spent re-calibrating the protocol for use with the particular cells. Future use of an updated protocol will give conclusive results.

MATERIALS AND METHODS

Bacterial Isolates

Both prokaryotic and eukaryotic cells were used for experimentation. Cell isolates were used for bacterial and co-culture experiments; a complete list of isolate origin and designation can be found below in Table 1.

Table 1: Isolates Used For Experimentation

Domain	Genus	Species	Cell Type	Origin	Designation
Eukaryote	*Mus*	*musculus*	Endothelial	Derived from mouse hemangioendo-thelioma ATTC CRL-2586	EOMA
Prokaryote	*Cronobacter*	*sakazakii*	Bacteria	Clinical Isolate from bison feces	52
Prokaryote	*Cronobacter*	*sakazakii*	Bacteria	Isolated from powdered infant formula ATTC BAA-894	BAA-894
Prokaryote	*Cronobacter*	*sakazakii*	Bacteria	Clinical isolate from cerebral spinal fluid of infant	CT2
Prokaryote	*Cronobacter*	*sakazakii*	Bacteria	Clinical isolate from bovine feces	N72 1A
Prokaryote	*Escherichia*	*coli*	Bacteria	ATTC 11775	K1
Prokaryote	*Escherichia*	*coli*	Bacteria	DH5α	DH5 α
Prokaryote	*Salmonella*	*enterica*	Bacteria	ATTC BAA-664 (Braenderup)	BAA-664

Growth Conditions

Bacterial Isolates

All bacterial isolates were maintained as freezer stock in 900 µl LB with 600 µl of 50% glycerol at -80 C. For experimental use of desired freezer stock, an isolation streak onto Luria Bertani (LB) agar plates was performed. LB plates were incubated at 37^{o}C overnight.

For the Antibiotic Disc Diffusion Assay, isolated bacterial colonies were picked and transferred to 3 ml LB broth and allowed to grow to an $OD_{600} \approx 0.2$-0.25 and plated on Mueller-Hinton Agar. For Cytoxicity Assays, bacterial isolates were plated onto MacConkey Agar (MAC) plates for differentiation . For Supernatant and Gentamicin/Adhesion Assays, a single colony of each desired bacterial isolate was picked off of each LB plate and transferred to 5 ml LB broth. Cultures were incubated overnight with shaking at 150 rpm. During Growth Curve Experiments, bacteria were incubated in 1ml LB broth at 37^{o}C for up to 48 hours. For Motility Assays, single colonies were removed from LB plates and inoculated onto motility plates. All media and reagents used for the bacterial experiments are included in Table 2.

Cell Culture

Endothelial cells were maintained in T-75 cell cultures flasks with Complete Dulbeco's Modified Eagle's Medium (C-DMEM) with 5% CO_2 at 37^{o}C. Cell culture lines were maintained for up to 64 passages. For long term storage, freezer stocks were maintained with 95 % C-DMEM and 5% DMSO in liquid nitrogen.

For Cytotoxicity and Supernatant assays, endothelial cells were grown to confluency on chamber slides and stored at 5% CO_2 and 37^{o}C for up to 48 hours. Endothelial cells were grown on 6-well plates for the Gentamicin/Adhesion Assays and stored under the same conditions for 2-24 hours. Media and reagents used for co-culture experiments are described in Table 2.

Media and Reagents

Table 2: Media and Reagents

Name	Abbreviation	Composition
1 X Phosphate Buffered Saline (Cell Culture Grade)	1X PBS	Not Available
Amikacin**	AN--30	30 ug disc potency
Amoxicillin/Clavulanic Acid**	Amc-30	20/10 ug disc potency
Ampicillin**	AM- 10	10 ug disc potency
Ceftiofur**	XNL-30	30 ug disc potency
Cephalothin	CF-30	30 ug disc potency
Chloramphenicol**	C-30	30 ug disc potency
Diff-Quick Stain Kit	Diff-Quick	Sln 1: 3.7% Formaldehyde,90% Methanol
Diff-Quick Stain Kit	Diff-Quick	Sln 2: .1%Azure II,.1% Phenothiazin-5-ium, 3,7-bia(dimethylamino)-chloride, 1% sodium phosphate monobasic monohydrate, 1%sodium phosphate, dibasic, anhydrous
Diff-Quick Stain Kit	Diff-Quick	Sln 3: .1% Eosin Y, .7% Sodium phosphate monobasic monohydrate, .3% sodium phosphate, dibasic, anhydrous
Dulbeco's Modified Eagle's Medium	DMEM	4 mM L-glutamine, 4500 mg/L glucose, 1 mM sodium pyruvate, and 1500 mg/L sodium bicarbonate
Fetal Bovine Serum	FBS	Not Available
Gentamicin**	GM 10	10 ug disc potency
Hematoxylin		<.6% hematoxylin powder, <30% Ethylene glycol, <5% Aluminum sulfate, <.1% Sodium iodate, <.2% Hydrochloric acid, <5% Aluminum ammonium sulfate
Kanamycin**	K -30	30 ug disc potency
Luria Bertani broth and agar	LB	1% Tryptone, 0.5% Yeast Extract, 1% NaCl
MacConkey Agar	MAC	0.017% Pancreatic digest of gelatin, 0.003% Peptone, 0.01% Lactose,0.0015% Bile Salts #3, 0.05% NaCl, 0.0135% agar, 0.000003% Neutral Red, .0000001% Crystal Violet
Motility Agar*		1% Tryptone , 0.5% NaCl, 0.3% agar
Mueller Hinton Agar		0.0175% Casein hydrolysate, 0.0015% Starch, 0.002% Beef Infusion Solids, 1.7% Agar
Nalidixic Acid**	Na-30	30 ug disc potency
Streptomycin**	S-10	10 ug disc potency
Sulfisoxazole**	G .25	250 ug disc potency
Tetracycline**	TE-30	30 µg disc potency
Tousimis Glutaraldehyde		2.5% in .1 M Na/K Sorensen's Phosphate buffer
Trypsin-EDTA		0.05% Trypsin and 0.02% EDTA
Lyse Solution***		2.5% Trypsin, .1% Triton-X, 80% PBS
Gentamicin		10mg/mL

All chemical and reagent information was found in MSDS unless otherwise noted.

***** (62) ** (63) ***(64)

Bacterial and Co-Culture Experiments

Growth Curve

Growth curves were performed utilizing a single colony of each bacterial isolate in 3ml of LB. Tubes were incubated overnight at 37^{o}C with shaking at 140 rpm. Overnight cultures were then diluted 1:100 and dispensed into 1.5 ml microfuge tubes which were stored at 37^{o}C. OD_{600} readings were taken hourly from hour 0 to 8 and then at hours 12, 24, and 48 with an Eppendorf BioPhotometer (Hamburg, Germany). A dilution series was performed for each hourly sample to determine the CFU/ml. Two replicates were performed for each bacterial isolate. To analyze the data, the averages and standard deviations were calculated for OD_{600} and CFU/ml data, separately for each bacterial isolate and time point. The two data sets were then graphed on a scatterplot with OD_{600} readings vs time on a logarithmic scale and CFU/ml vs time on a linear scale. The doubling time for each isolate was determined by using CFU/ml corresponding to the log phase of each growth curve. The doubling time for each isolate was calculated using the following formula: G= t/3.3 logb/B (65). Where: G represents generation time, t represents time in minutes, b represents the number of bacteria at the end of the time interval, and B represents the number of bacteria at the beginning of the time interval.

Antibiotic Susceptibility Testing

To determine the susceptibility of each bacterial isolate to 12 different antibiotics, the Kirby-Bauer disc diffusion method was used with 150 X 15 mm Mueller-Hinton agar plates (63). Prior to testing, each bacterial isolate was incubated in 3 ml of LB until an $OD_{600} \approx 0.2$-0.25 was reached. Sterile swabs were then used to inoculate bacteria from the liquid cultures onto Mueller-Hinton agar plates, spreading the bacteria across the entire surface of the plate. After inoculation,

antibiotic discs were dispensed onto individual agar plates. Following overnight incubation at 37^{o}C, antibiotic susceptibility was determined by measuring the zone of inhibition for each antibiotic and bacterial isolate. One replicate was performed for each sample. BIOMIC 2010 software and the Kirby-Bauer XNL program were utilized for analysis. The software distinguished between three categories of antibiotic susceptibility: susceptible, intermediate, and resistant. The zones that separate these categories are characteristic for each antibiotic. The software compared the measured inhibition zones to these standard inhibition zones to categorize the isolates with respect to the different antibiotics.

Motility

The motility of each bacterial isolate was determined at 25^{o}C and 37^{o}C using 150 x 15 mm motility plates. Single colonies were inoculated into the center of each plate and the diameter (in mm) of the growth rings were measured hourly until they reached the edge of the plate. Three replicates were performed for each bacterial isolate. To analyze the data, the averages and standard deviations of the diameters were calculated across the replicates for each bacterial isolate. The growth ring data were then plotted in mm diameter vs time in hours on a linear scale. The rate of movement was determined for each isolate by determining the linear regression of the growth ring data. Data are expressed in mm/hr.

Chamber Slide Assays

All chamber slides were inoculated with EOMA cells, which were allowed to grow to confluency prior to experimental inoculation with bacterial isolates.

Cytotoxicity Assay

Bacterial isolates were grown overnight in LB broth at 37^{o}C 150 rpm. Each isolate was then diluted and 10^{8} cfu/mL were pipetted into the chamber slides with the confluent monolayer of EOMA cells. Co-cultures of bacterial and EOMA cells were incubated at 37^{o}C and 5% CO_2 for 24, 36, & 48 hours. After incubation, the supernatant from each isolate was plated onto MacConkey agar and chamber slides were processed with glutaraldehyde. Cells were stained with hematoxylin or Diff-Quick, and viewed under an Olympus BX61 bright field microscope (Center Valley, PA) at 200 x, 600 x, and 1000 x magnification. Three replicates were performed for each bacterial isolate co-cultured with the EOMA at each time point. Representative images were taken for each bacterial isolate producing between 25-30 images per isolate at each time point. Data were qualitatively analyzed and one representative image is shown per bacterial isolate (in co-culture with the EOMA cells) and time point.

Supernatant Assay

Bacterial isolates were grown in LB overnight. Supernatants were obtained by centrifuging the overnight cultures at 4000 rpm for 10 minutes at 25C. The supernatant of each isolate was filtered through a 3 micron filter and inoculated on top of the confluent monolayer of EOMA cells in the chamber slides. Chamber slides were incubated at 37^{o}C at 5% CO_2 for 24, 36, & 48 hours. Live views of co-cultures were taken on a Zeiss AxioObserver Z1, and PlasDIC set, equipped with with Zeiss HRc Rev3 color camera and Zeiss AxioVision Rev. 4.8.1 microscope control software. (Zeiss Microimaging, Thornwood NY). All images were taken at 200x. Three replicates were performed for each supernatant at each time point. Representative images were taken for each sample producing between 25-35 images per isolate at each time point. Data were

qualitatively analyzed and one representative image is shown per supernatant (in co-culture with the EOMA cells) and time point.

Gentamicin and Adhesion Assays

Assays were prepared by growing a confluent monolayer of EOMA cells in 6-well plates. All plates were stored at 37^{o}C and 5% CO_2. The assay was performed as described by Berry et al, 2009 (64).

Gentamicin Assay

Each bacterial isolate was aseptically inoculated into individual wells of the plate at a multiplicity of infection of 10. The plates were then centrifuged at 600x gravity for 2.5 minutes twice. After centrifugation to enhance bacterial and EOMA cell contact, plates were incubated at 37^{o}C for two hours. Gentamicin was then added to each well and plates were inoculated for an additional half hour. Following the final incubation, each well was washed with 4mL PBS and EOMA cells were then lysed with the lyse solution described in Table 1. A dilution series was performed for the contents of each well and all dilutions were plated on LB to enumerate the number of colony forming units of each isolate in all wells. The number of cfu/ml of each isolate represents the number of intracellular bacteria for each well. This number can then be compared to the number of total bacteria in each well (determined in the Adhesion) to calculate the percent invasion of EOMA cells for each isolate.

Adhesion Assay

Each bacterial isolate was aseptically inoculated into individual wells of the plate at a multiplicity of infection of 10. The plates were then centrifuged at 600x gravity for 2.5 minutes

twice. After centrifugation to enhance bacterial and EOMA cell contact, plates were incubated at 37^{o}C for two hours. Each well was washed with 4mL PBS and EOMA cells were then lysed with the lyse solution described in Table 1. A dilution series was performed for the contents of each well and all dilutions were plated on LB to enumerate the number of colony forming units of each isolate in all wells. The number of cfu/ml of each isolate represents total number of bacteria that remain attached plus the number that have invaded the EOMA cells. This number can then be used to calculate percent invasiveness for each isolate as described above in the Gentamicin Assay.

RESULTS

Antibiotic Susceptibility of the Bacterial Isolates

In order to validate the use of the bilayer blood brain barrier system and the pathogenesis caused by bacteria, individual *E. coli* and *C. sakazakii* bacterial isolates listed in Table 1 were first characterized to ensure they represent properties as previously described. Antibiotic susceptibility testing, growth curves, and motility analysis were performed to gain a preliminary understanding of both the control and test organisms' physical and chemical properties.

Antibiotic susceptibility testing was performed using the disc diffusion method and representative drugs from the following drug classes: aminoglycoside, cephalosporin, chloramphenicol, penicillin, quinolone, sulfonamide, and tetracycline. Individual 150 mm plate with Mueller-Hinton agar plates were aseptically inoculated with the control strains of *E. coli* and test strains of *C. sakazakii* using cultures standardized to an $OD_{600} \approx .2$-25. After completely covering each plate with an individual strain of bacteria listed below in Table 3, twelve different antibiotic discs (BD BBL Sensi-Disc, Maryland) were added to each plate and grown overnight at 37^{o} C. Plates were then analyzed with BIOMIC 2010 software utilizing the Kirby-Bauer-XNL program to assess zones of inhibition. Results are shown below in Table 3.

The cytotoxicity and supernatant assay control strains of *E. coli*, DH5 α and K1, both showed sensitivity to all antibiotics tested, with the exception of nalidixic acid (NA-30). DH5 α showed an intermediate susceptibility to this nucleic acid disrupting quinolone. DH5α is a non-pathogenic K12 strain of *E. coli* that is sensitive to most antibiotics; this strain is unable to colonize intestines and lacks most virulence factors (66, 67).The findings from this antibiotic screen, agree with this data. *E. coli* K1 strains have been shown to be sensitive to ampicillin,

chloramphenicol, and gentamicin (68). The K1 strain used in this study is also sensitive to these drugs.

The *C. sakazakii* isolates used in this study were uniformly resistant to cephalothin (CF-30) and uniformly sensitive to all other antibiotics tested including: gentamicin (Gm-10), ampicillin (Am-10), chloramphenicol (C-30), kanamycin (K-30), and streptomycin (S-10). These results agree with literature findings that *C. sakazakii* is sensitive to gentamicin, ampicillin, chloramphenicol, kanamycin, and streptomycin and others while showing resistance to beta lactam drugs such as cephalothin(3, 19, 32, 37) .However, some strains of *C. sakazakii* have been found to be resistant to tetracycline (Te-30), which is not consistent with this study (19).

Table 3: Antibiotic Susceptibilities

Isolate	Te-30	Amc-30	C-30	Gm 10	Ceftiofur	CF-30	K-30	S-10	Am-10	An-30	Sulfisoxazole	Na-30
DH5α	S	S	S	S	S	S	S	S	S	S	S	I
K1	S	S	S	S	S	S	S	S	S	S	S	S
52	S	S	S	S	S	R	S	S	S	S	S	S
BAA 894	S	S	S	S	N/A	R	S	S	S	S	N/A	S
CT2	S	S	S	S	S	R	S	S	S	S	S	S
N72	S	S	S	S	S	R	S	S	S	S	S	S

Bacterial Growth

Experimental procedures for the cytotoxicity and supernatant assays were carried out under static conditions at 37^{o} C and 5% CO_2. In order to approximate the growth rate of the bacteria in LB broth under these conditions, the OD_{600} of individual isolates was measured hourly when kept at static conditions and 37^{o} C. Plates counts were also taken hourly to assess the doubling time of bacteria.

The negative *E. coli* control DH5 α shows a delayed lag phase when compared to the positive K1 control as seen in Figure 2 below. Both isolates show normal growth curves with characteristic log and stationary phases. The doubling time for each strain was calculated using the equation : G= t/3.3 logb/B where: t equals time, b equals number of bacteria at endpoint, and B equals number of bacteria at startpoint (65). According to plate count data used with these calculations, under static growth at 37 ^{o} C *E. coli* DH5 α doubles approximately every 31 minutes while K1 doubles approximately every 43 minutes. The calculated doubling times do not agree with the appearance of the growth curve which suggests the K1 isolate grows at a faster rate than the DH5 α. This discrepancy is most likely due to plating inefficiency of dilutions used. The Bacterial Analytic Manual (BAM) recommends that plate counts between 25-250 colony forming units (cfu) be used for best results; most statistical analysis uses an n of 30 as a statistically significant figure (69, 70). Despite plating multiple dilutions, colony counts within the accepted range were not always found; some results report fewer than 25 cfu/ml. This could greatly affect the accuracy of the plate counts and account for the seemingly disparate doubling times. Overall, the estimated doubling times of both *E. coli* strains in this study remain within the same time frame of the accepted doubling time of *E. coli* under optimal conditions with shaking

which is 20 minutes (61). The longer doubling time is expected as the optimal doubling time of *E. coli* is calculated with shaking, whereas this study used static conditions which results in a loose pellet at the bottom of culture tubes versus a homogenous mixture throughout the tube.

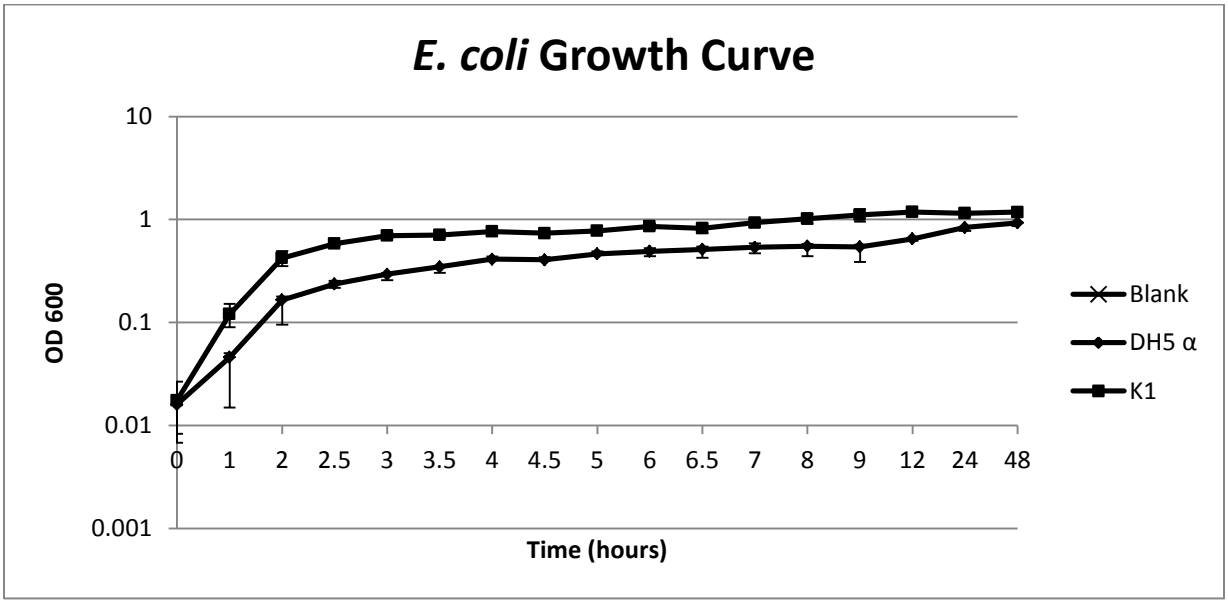

Figure 2: *E. coli* Growth Curve at 37^{o} C in LB Broth Under Static Conditions. The X axis measures time in hours and the Y axis represents the OD_{600} reading on a logarithmic scale. The K1 isolate quickly moves into log and stationary phase. DH5 α shows a similar growth pattern with delayed lag and log phase in comparison to K1.

The *C. sakazakii* experimental isolates 52, BAA 894, CT2, and N72 all show uniform growth curves that tightly cluster between isolates as shown in Figure 3 below. The calculated doubling times of the isolates are as follows: Isolate 52, approximately 16 minutes; BAA 894, approximately 12.5 minutes; CT2, approximately 14 minutes; and N72, approximately 17 minutes. These doubling time values are likely an underestimation of the true doubling time as the plate count method did not always produce cfus in the countable range which forced the use of colonies counts under 25. Iverson et al report that *Cronobacter Complex*have an average doubling time of 22 minutes at 37^{o} C (17) . The *C. sakazakii* doubling time values reported

above fall closely within this range. The discrepancy between the reported doubling time and those found in literature of *E. sakzakii* (*Cronobacter* species) and the isolates used in this study are most likely due to plating inefficiency.

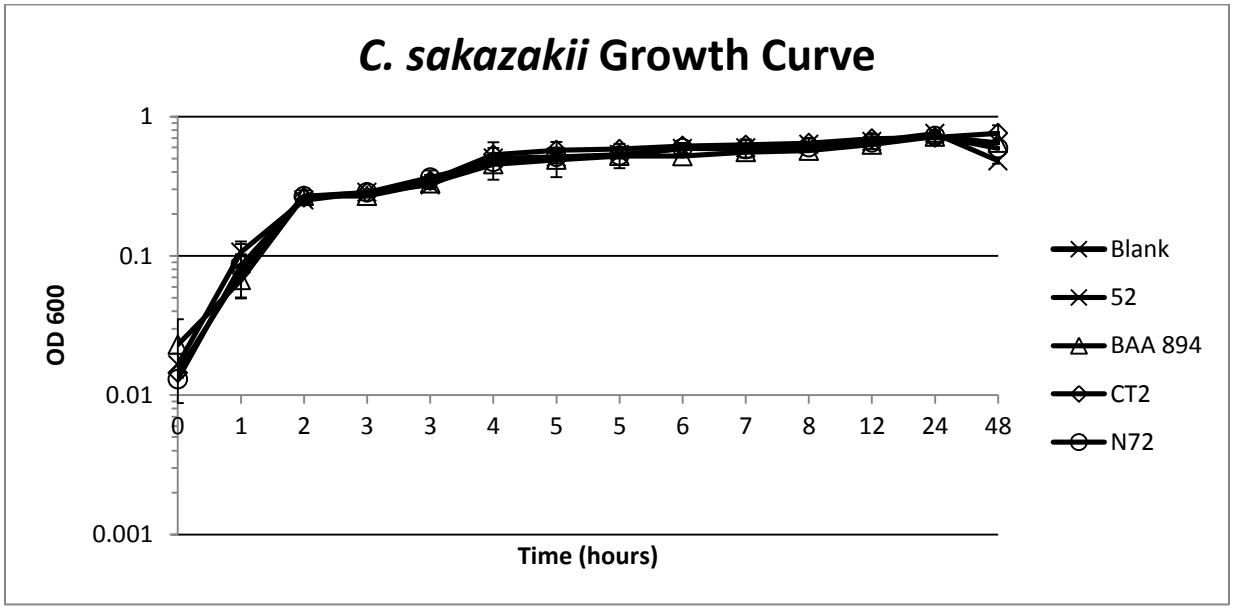

Figure 3: *C. sakazakii* Growth Curve at 37^{o} C in LB Broth Under Static Conditions. The X axis measures time in hours and the Y axis represents the OD_{600} reading on a logarithmic scale. All isolates appear to cluster closely showing uniform growth from lag and log phase into stationary phase.

Below, Figure 4 shows the combined growth curves of all *E. coli* and *C. sakazakii* isolates. The combined figure shows that the K1 isolate has a quicker growth rate than the clustered *C. sakazakii* isolates while the DH5 α isolate grows slowest. Again, the discrepancy between the calculated doubling times, which estimates a much faster doubling rate for the *C. sakazakii* isolates, is due to plating inefficiency; the OD_{600} readings plotted against time more accurately reflect the actual growth of the isolates.

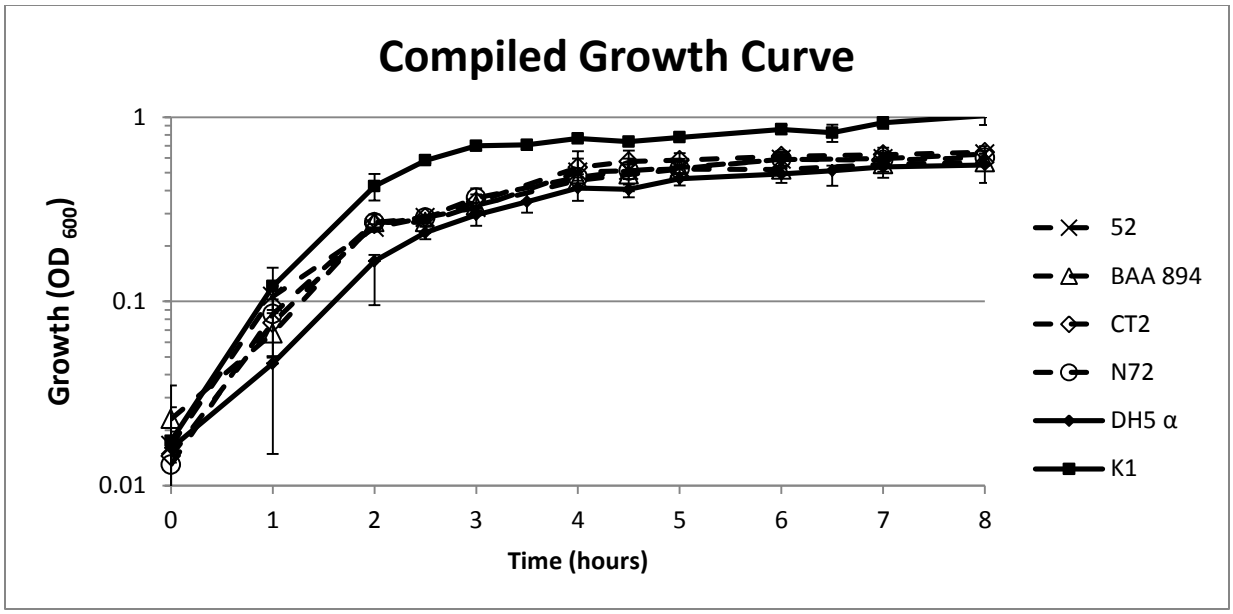

Figure 4: Combined Growth Curves of *E. coli* and *C. sakazakii* Isolates. The OD_{600} values are plotted on a logarithmic scale vs time in hours. All isolates show similar growth patterns with the positive K1 control showing a slightly increased rate and the negative DH5 α control showing a decreased rate of growth in log phase.

Both the *E. coli* isolates used as assay controls and the experimental *C. sakazakii* isolates used show standard growth patterns fall within the accepted doubling time ranges of their representative species. In terms of growth, all isolates were deemed to grow at similar rates. This excludes slow growth as a reason for differences seen between cytotoxicity over time.

Bacterial Motility

To further characterize *E. coli* and *C. sakazakii* isolates, bacterial motility was analyzed at two temperatures 25^{o} C and 37^{o}C. Bacterial movement in motility agar gives an indirect method to determine whether flagella are expressed and allows calculation of movement rate in millimeters per hour. The expression of flagella may contribute to bacterial pathogenesis and further analysis can be performed to determine the structural role of these structures in contribution to disease. Motility was assessed using the swarm plate method as described by

Wolfe and Berg (62). Individual isolates were aseptically inoculated into the center of each motility plate and stored at 25° C and 37° C, respectively with swarming rings measured hourly.

The *E. coli* isolates show contrasting motility patterns as shown in Figure 5 Below. K1 exhibits motility at 25°C while DH5α is non-motile. The rates of motility for K1 and DH5α at 25° C are 2.74 mm/hr and 0 mm/hr, respectively.

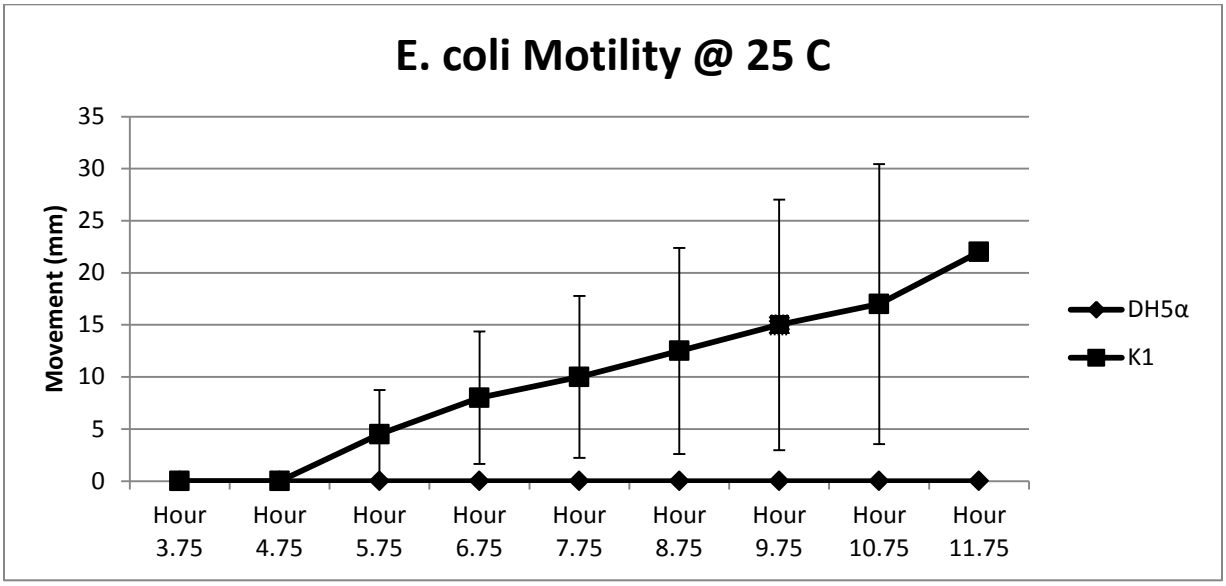

Figure 5: *E. coli* Motility at 25° C on Swarm Plates. Motility is plotted with movement in millimeters (mm) vs. time in hours. K1 shows motility at a rate of 2.74mm/hr while DH5α is non-motile.

C. sakazakii isolates were all found to be motile at 25° C, although rates of motility differed between strains. Figure 6 shows the variation between strains. Isolate motility at 25° C is as follows: 52: 2.43 mm/hr; BAA 894: 6.9mm/hr; CT2: 2.37 mm/hr; N72 1A: 2.925 mm/hr. BAA 894 shows the highest rate of motility at this temperature while the other isolates exhibit motility rates similar to *E. coli* K1 under the same conditions. *Cronobacter Complex* are generally motile (3, 4).

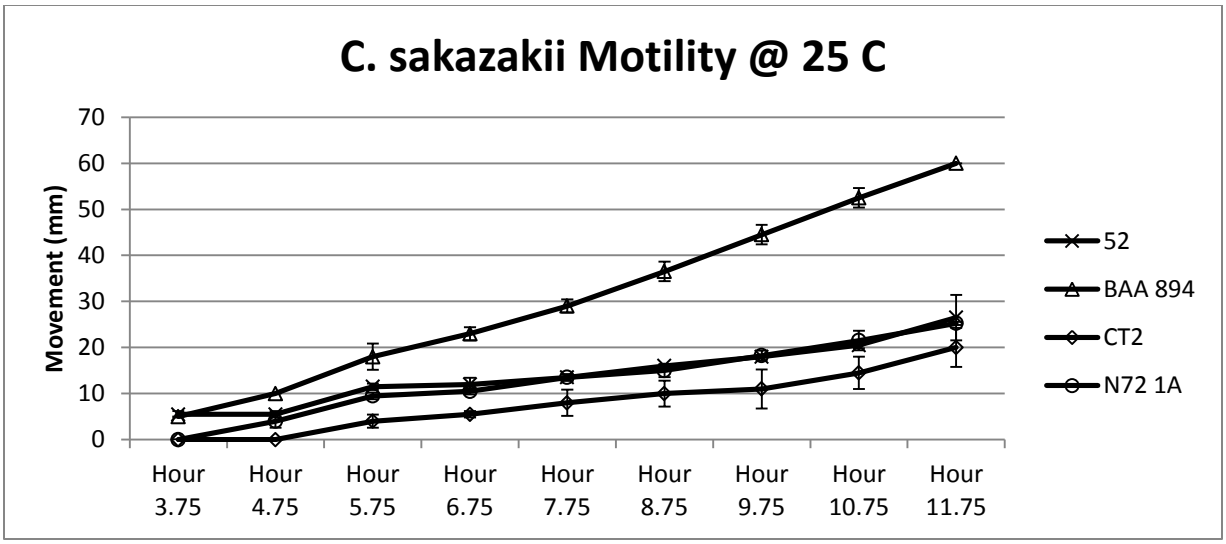

Figure 6: *C. sakazakii* Motility at 25^{o} C on Swarm Plates. Motility is plotted with movement in millimeters(mm) vs time in hours. All *C. sakazakii* isolates are motile at these conditions, with BAA 894 exhibiting the highest rate of motility at 6.9mm/hr.

The positive and negative *E. coli* controls show contrasting motility patterns at 37^{o} C as well, which can be seen in Figure 7. K1 exhibits motility while DH5α is non-motile. The rates of motility for K1 and DH5α at 25^{o} C are 4.34 mm/hr and 0 mm/hr, respectively.

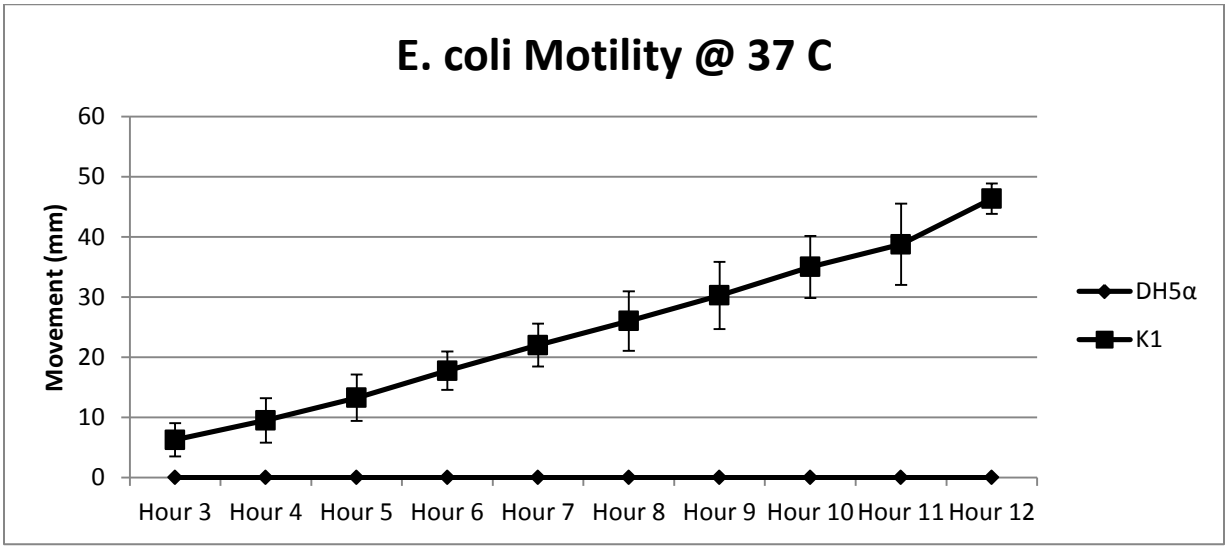

Figure 7: Figure 4: *E. coli* Motility at 37^{o} C on Swarm Plates. Motility is plotted with movement in millimeters (mm) vs. time in hours. K1 shows motility at a rate of 4.34 mm/hr while DH5α is non-motile.

C. sakazakii isolates were all found to be motile at 37^{o} C, although rates of motility differed between strains as seen in Figure 8. All isolates showed increased motility at this temperature compared to motility at 25^{o} C. Isolate motility at 37^{o} C is as follows: 52: 9.8 mm/hr; BAA 894: 15.44 mm/hr; CT2: 6.62 mm/hr; N72 1A: 13.33 mm/hr. BAA 894 again shows the highest rate of motility at this temperature with N72 1A also showing a similarly high rate. Isolates 52 and CT2 show lower rates of motility but these are still higher than that of *E. coli* K1 at the same temperature.

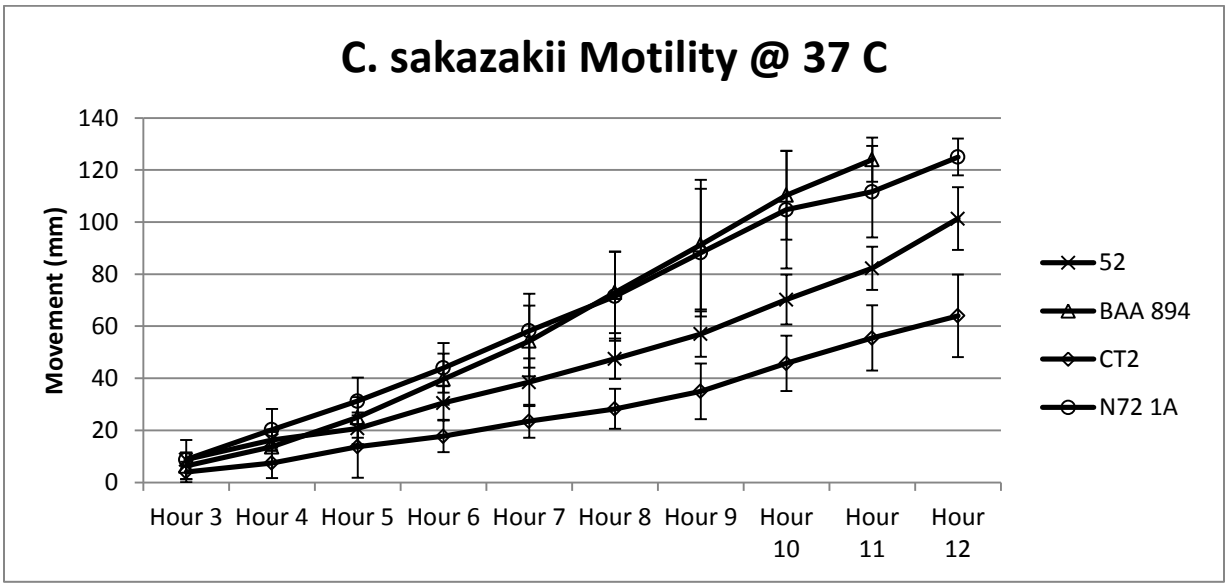

Figure 8: *C. sakazakii* Motility at 37^{o} C on Swarm Plates. Motility is plotted with movement in millimeters (mm) vs time in hours. All *C. sakazakii* isolates are motile at these conditions, with BAA 894 and N72 1A both exhibiting the highest rates of motility at 15.44 mm/hr and 13.33 mm/hr, respectively.

Cytotoxicity Assays

The cytotoxicity assays measured bacterial ability to disrupt and or damage the mouse endothelial cell line over a time course of 48 hours. Confluent endothelial (EOMA) cells were inoculated with 10^{8} cfu/ml from overnight bacterial cultures. Different bacterial isolates were pipetted into individual chambers of the chamber slide and all chamber slides were incubated at

37°C 5% CO_2. Slides were processed and stained at three time points, 24 hours, 36 hours, and 48 hours, and stained with either diff-quick or hemotoxylin. All slides were viewed on a bright field microscope and imaged at 200x, 600x, and 1000x magnification. Representative images from the larger 200x field of view are shown in the following figure to illustrate EOMA confluency and cell morphology after incubation with bacterial isolates.

E. coli K1 was used as a positive control while DH5 α served as the non-pathogenic negative control. *C. sakazakii* isolates 52, BAA 894, CT2, and N72 1A were used to assess damage to EOMA cells. With respect to damage to EOMA cells, relative confluency and morphology of the EOMA cells is qualitatively compared. The bacterial aggregation patterns and changes in EOMA cell morphology were compared between control and test isolates. At the initial 24 hour time point, *C. sakzakii* isolates show very little damage to EOMA cells and most closely resemble the DH5 α control. However, the *C. sakazakii* isolates showed increased damage to EOMA cells over time, showing similar levels of damage at 48 hours as the K1 control.

Figures 9-14 below show EOMA cell controls, *E. coli* positive and negative controls, and *C. sakazakii* test isolates.

Figure 9 shows that the DH5 α negative control shows no apparent damage to EOMA cells at any time point. The EOMA cells remain 100% confluent and retain normal cell morphology.

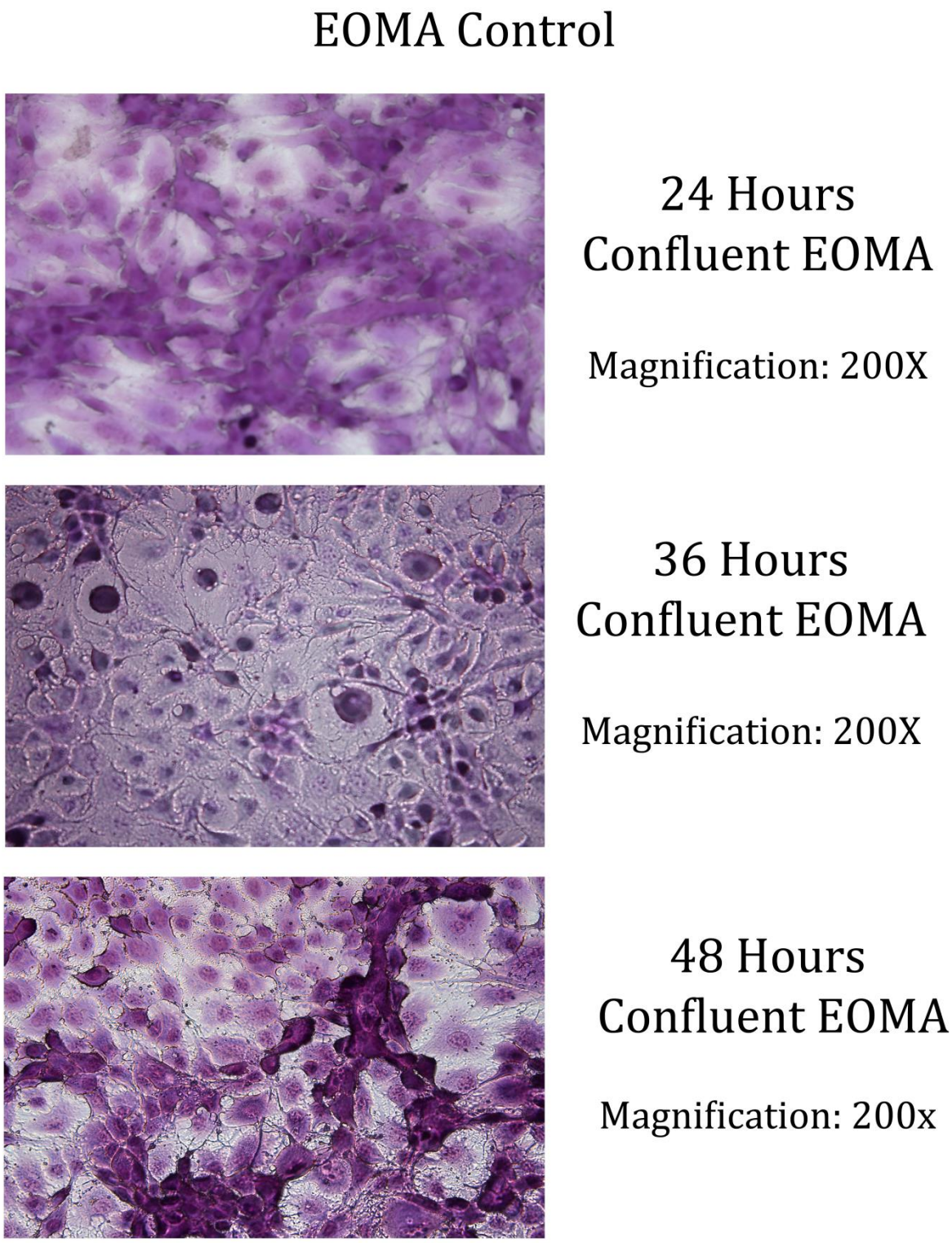

Figure 9: EOMA Cytotoxicity Assay Control. A confluent monolayer of EOMA cells at 24, 36, and 48 hours at 200X magnification. Cells remain 100% confluent and retain normal morphology.

In Figure 10, the *E. coli* cytotoxicity patterns can be seen for both the positive and negative meningitis causing controls.The positive K1 control shows increasing damage to EOMA cells at all time points investigated. Initially, at 24 hours, EOMA cells show reduced confluency and the cells begin to show a rounded morphology and K1 cells can be seen in both cell-free areas and clustered on top of remaining cells. At 36 hours, cell confluency is further reduced and K1 cells cover a majority of the slide surface obscuring remaining EOMA cells; cell confluency remains around 75%. At 48 hours, EOMA cell confluency is reduced to approximately 25%. Again, K1 cells appear clustered in both cell-free areas and aggregated over the remaining EOMA cells.

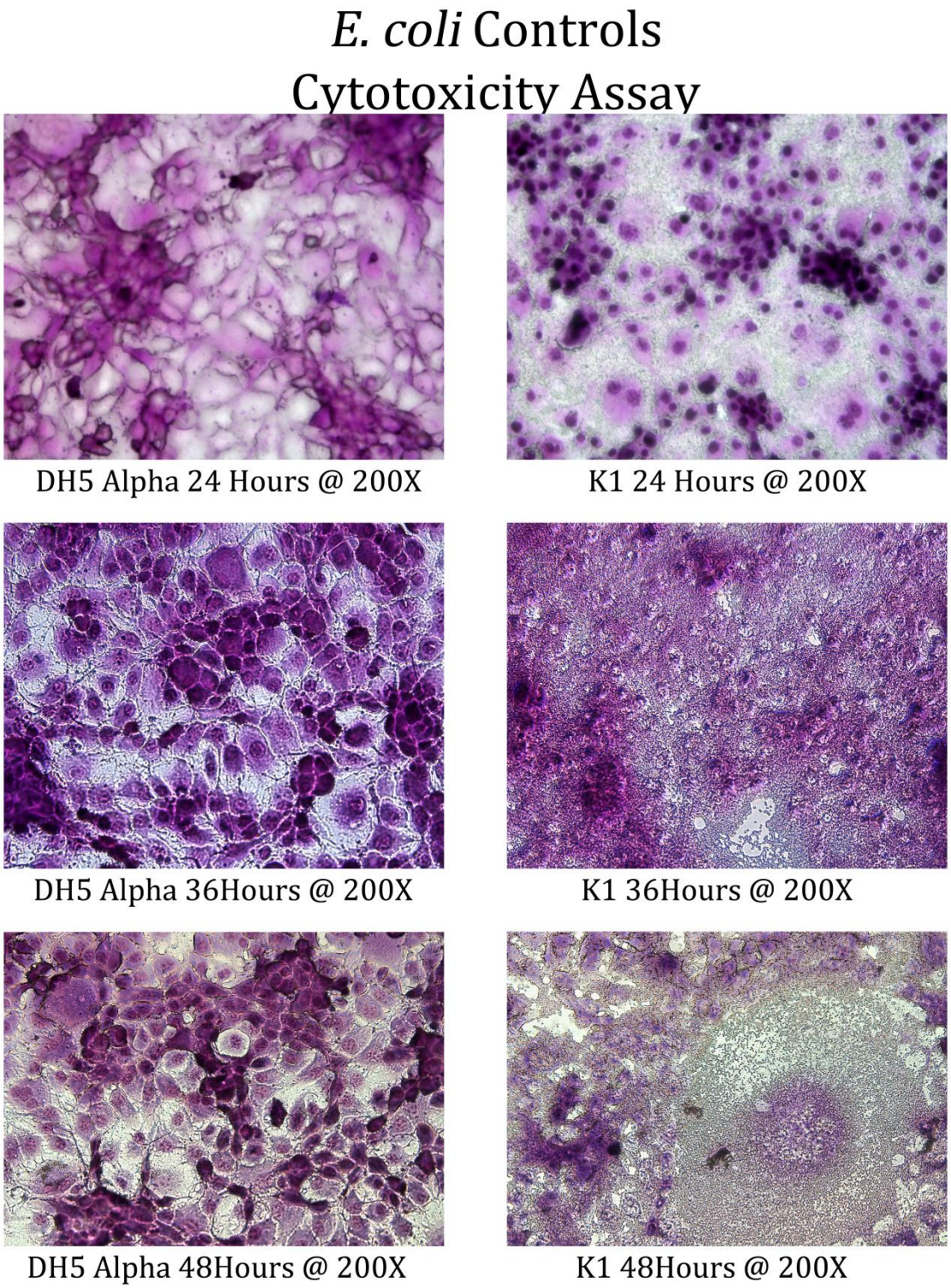

Figure 10: *E. coli* Cytotoxicity Assay Control. The left panel shows DH5α at 24, 36, and 48 hours at 200X magnification; the right panel shows K1 at the same time points and magnification.

Below, Figure 11 shows *C. sakazakii* BAA 894 in the right-hand panel at each time point. K1 is shown on the left at corresponding time points for comparison. Initially, no apparent damage is seen at the 24 hour time point. The EOMA cells remain 100% confluent with normal cell morphology. However, after 36 hours BAA 894 shows significant damage to the EOMA cells. EOMA confluency is reduced below 50% and remaining cells begin to show rounding. BAA 894 cells can be seen aggregated around EOMA cells and dispersed in cell free areas. At this time point, the BAA 894 isolate shows more damage than the K1 positive control, which did not decrease EOMA confluency below 50%. In addition, the bacteria appear to behave differently when in contact with EOMA cells. The K1 control aggregates on top of and around the EOMA cells while BAA 894 aggregates around EOMA cells only. At 48 hours BAA 894 reduces EOMA cell confluency below 25% leaving remaining EOMA cells with abnormal and rounded morphologies. Again, the damage caused by BAA 894 is more severe than that of the K1 control. BAA 894 cells can still be seen near EOMA cells, although clustering is not as evident. Few cells remain on the slide. In contrast, the K1 cells still aggregate on top of an around EOMA cells and show great cell numbers throughout the slide at 48 hours.

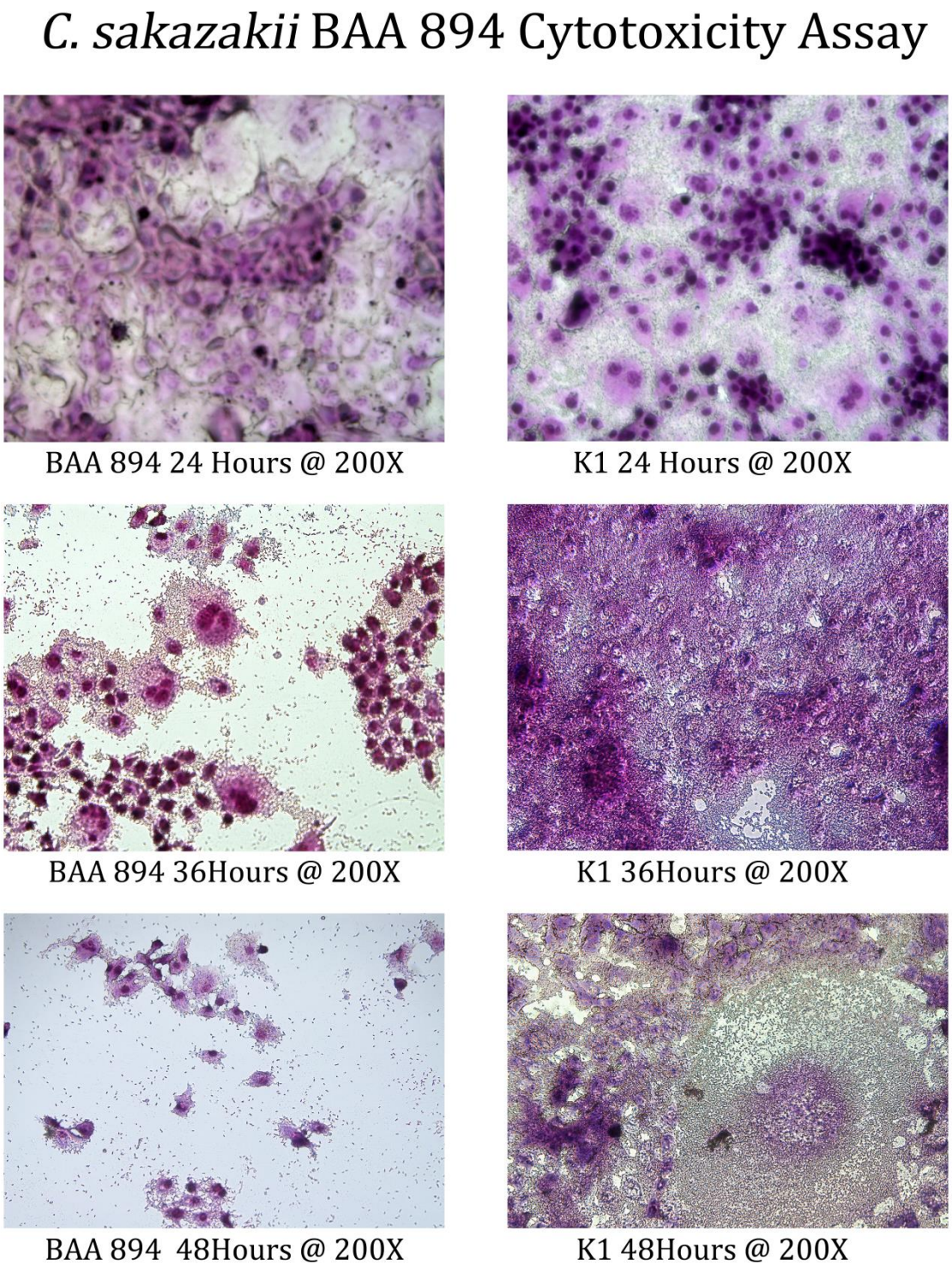

Figure 11: BAA 894 Cytotoxicity Time Course**.** The panel on the left shows *C. sakazakii* BAA 894 at 24, 36, and 48 hours at 200X magnification; the right panel shows K1 at the same time points and magnification.

Figure 12 shows *C. sakazakii* 52 in the right-hand panel at each time point. K1 is shown on the left at corresponding time points for comparison. This isolate initially shows no apparent damage or reduction in EOMA confluency at 24 hours but begins to show increasing adverse effects after 36 and 48 hours. At 36 hours, isolate 52 causes a reduction in EOMA cell confluency similar to that of K1 at the same time point: approximately 75% confluency. EOMA cells begin to show more rounded morphology. At 36 hours isolate 52 cells appear to both aggregate on top of and around the EOMA cells in a similar fashion to K1. Some cells can be seen diffused in cell-free spaces. At 48 hours, isolate 52 reduces EOMA cell confluency below 25% similar to K1. Here, isolate 52 cells aggregate around and on top of EOMA cells with some aggregated cells in EOMA cell-free areas.

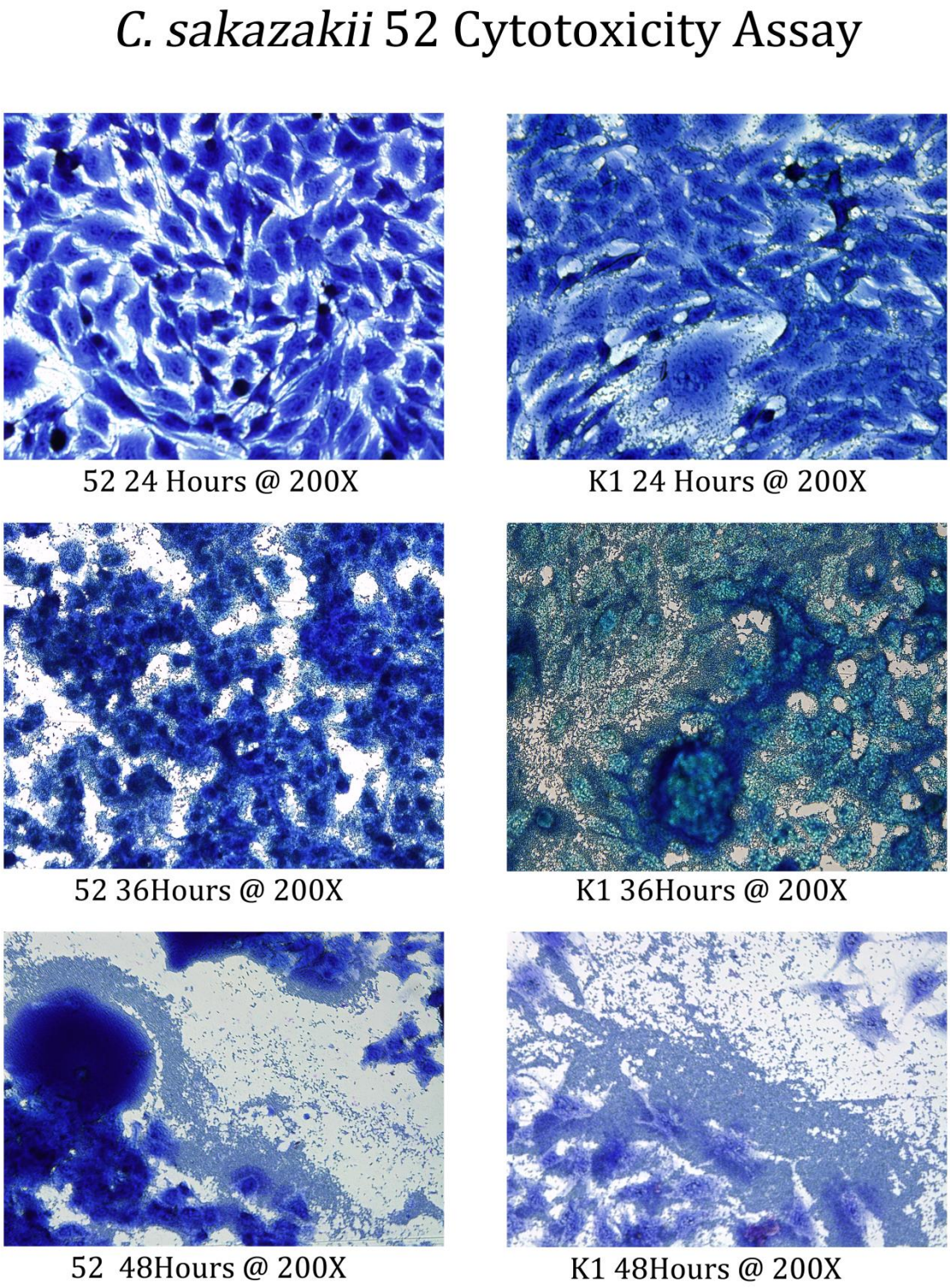

Figure 12: 52 Cytotoxicity Time Course. The panel on the right shows *C. sakazakkii* 52 at 24, 36, and 48 hours at 200X magnification; the right panel shows K1 at the same time points and magnification.

Figure 13 shows *C. sakazakii* CT2 in the right-hand panel at each time point. K1 is shown on the left at corresponding time points for comparison. The results in this time course are not as consistent as those of other *C. sakazakii* isolates. At 24 hours, no apparent EOMA cell damage can be seen when inoculated with CT2. After 36 hours, a high degree of damage is seen with EOMA cell confluency reduced below 50%. Remaining EOMA cells are obscured by CT2 cells aggregated around and on top of the EOMA monolayer. At this time, CT2 causes a greater reduction in EOMA cell confluency than K1. However, this isolate showed varying results between experimental repetitions with some trials showing high degrees of damage at 36 and 48 hours while showed none. The 48 hour time point shown in Figure 13 represents an experimental run where little to no damage was seen even after 48 hours. The EOMA monolayer remains nearly 100% confluent with normal cell morphology.

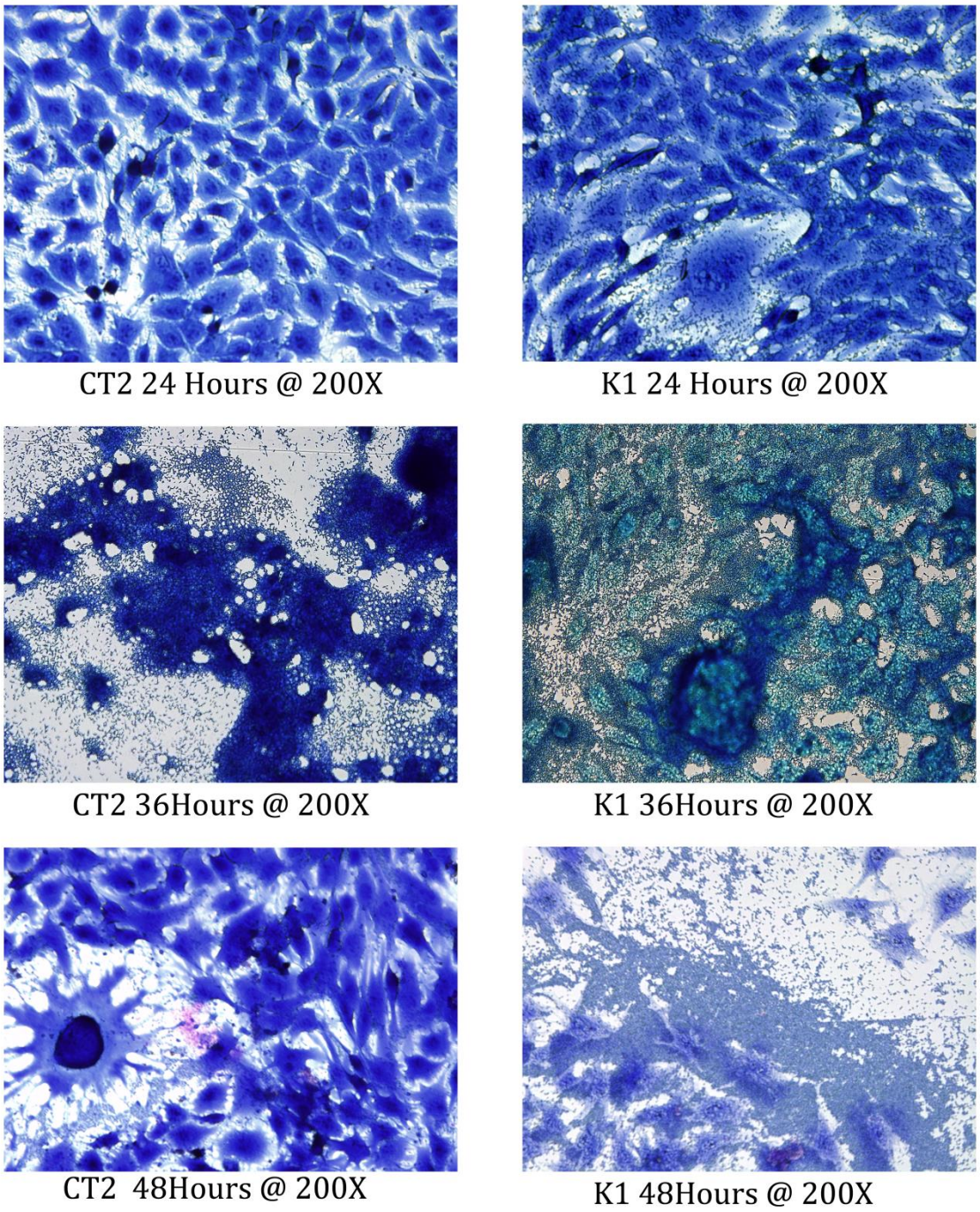

Figure 13: CT2 Cytotoxicity Time Course**.** The panel on the right shows *C. sakazakkii* CT2 1A at 24, 36, and 48 hours at 200X magnification; the right panel shows K1 at the same time points and magnification.

Figure 14 shows *C. sakazakii* N72 1A in the right-hand panel at each time point. K1 is shown on the left at corresponding time points for comparison. The results in this time course show increasing pathogenic effects after 36 hours with damage similar to the K1 control. At 24 hours, no apparent EOMA cell damage can be seen when inoculated with N72 1A. After 36 hours, damage to EOMA cells can be seen in terms of a reduction in confluency, changes in cell morphology, and high numbers of bacterial cells. The EOMA cell monolayer shows a slight reduction, but remains over 75% confluent. N72 1A cells appear to stack on top of and clustered around the EOMA cells. At 48 hour time point, a greater reduction in EOMA cell confluency can be seen. EOMA cells show 50% confluency as compared to 25% confluency with the K1 control. In both the N72 1A and K1 48 hour time points EOMA cells show great cell rounding and reduced cell-cell contact. Bacterial cells appear to cluster on top of and clustered around the remaining cells in the monolayer.

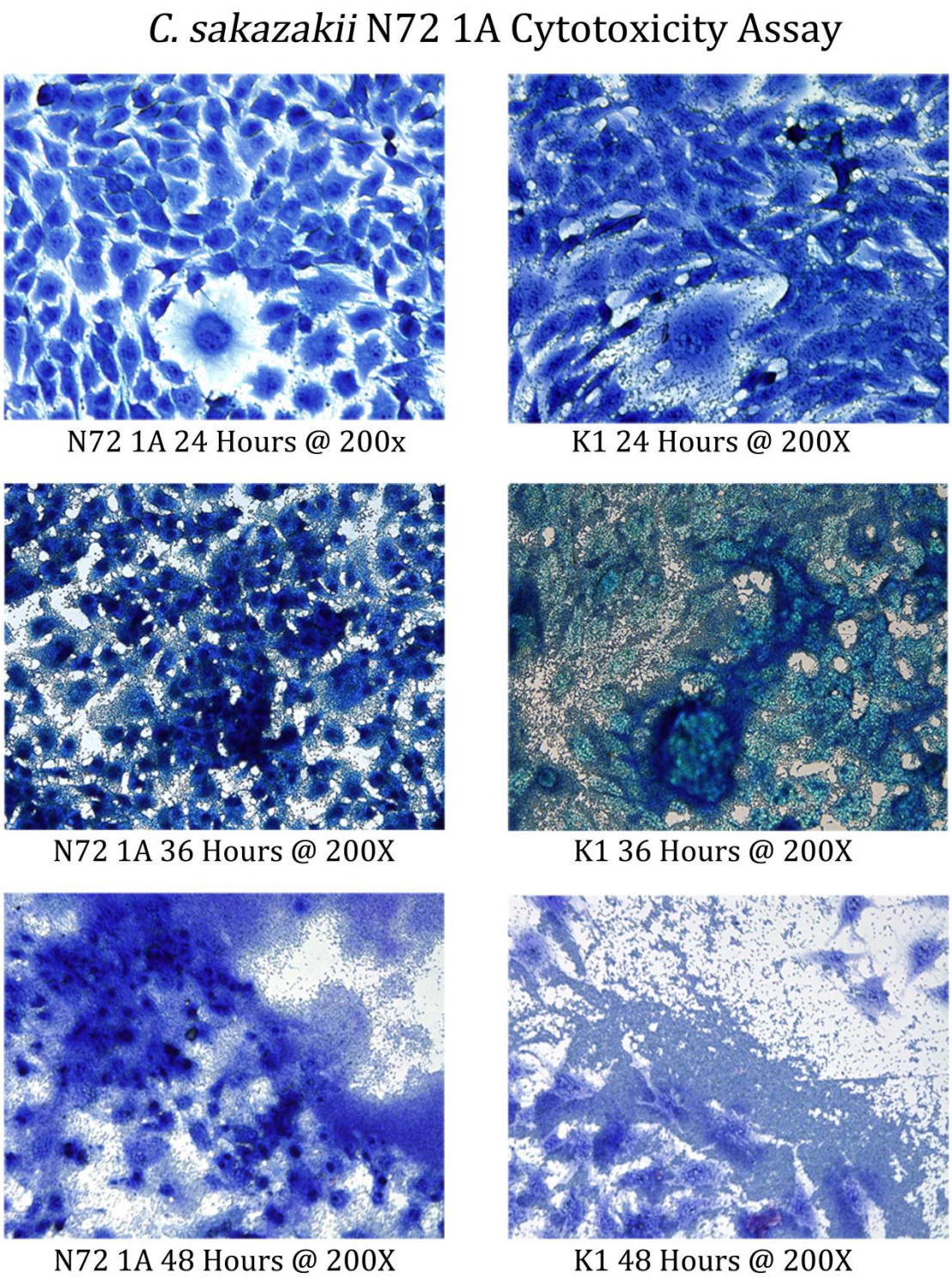

Figure 14:N72 1A Cytotoxicity Time Course. The panel on the right shows *C. sakazakkii* N72 1A at 24, 36, and 48 hours at 200X magnification; the right panel shows K1 at the same time points and magnification.

Supernatant Assays

The supernatant assays measured bacterial ability to disrupt and or damage the mouse endothelial cell line over a time course of 48 hours using concentrated supernatant from individual overnight bacterial cultures in LB. Confluent endothelial (EOMA) cells were inoculated with 2 mls concentrated bacterial supernatant that was filtered through a 3 micron filter and syringe. Endpoint supernatant was plated to ensure that no live bacteria were present. Different supernatants from isolates were pipetted into individual chambers of the chamber slide and all chamber slides were incubated at 37^{o}C 5% CO_2. Slides were viewed live on a differential interference contrast (DIC) microscope at, 24 hours, 36 hours, and 48 hours. All slides were imaged at 200x magnification. Representative images from are shown in the following figure to illustrate EOMA confluency and cell morphology after incubation with bacterial isolates.

E. coli K1 was used as a positive meningitis-causing control while DH5 α served as the non-pathogenic negative control. *C. sakazakii* isolate BAA 894 was chosen to assess damage to EOMA cells due to its ability to reduce EOMA cell confluency to a high degree and because it is known to cause meningitis (71, 72). With respect to damage to EOMA cells, relative confluency and morphology of the EOMA cells is qualitatively compared. The EOMA cell morphology was also compared between control and test isolates. Both the supernatant-free EOMA cell control and the negative DH5 α control, seen in Figure 15, show now apparent damage to the monolayer of EOMA cells at any time point. The K1 negative control does not show damage to the monolayer early on (Figure 16), but after 36 hours, EOMA cell rounding and reduced confluency can be seen. At the Initial 24 hour time point the supernatant from BAA 894 (Figure 16) begins to show damage to the EOMA monolayer whereas the K1 control does not.

Figures 15-16 below show EOMA cell controls, *E. coli* positive and negative controls, and *C. sakazakii* BAA 894 at 24, 36, and 48 hour time points.

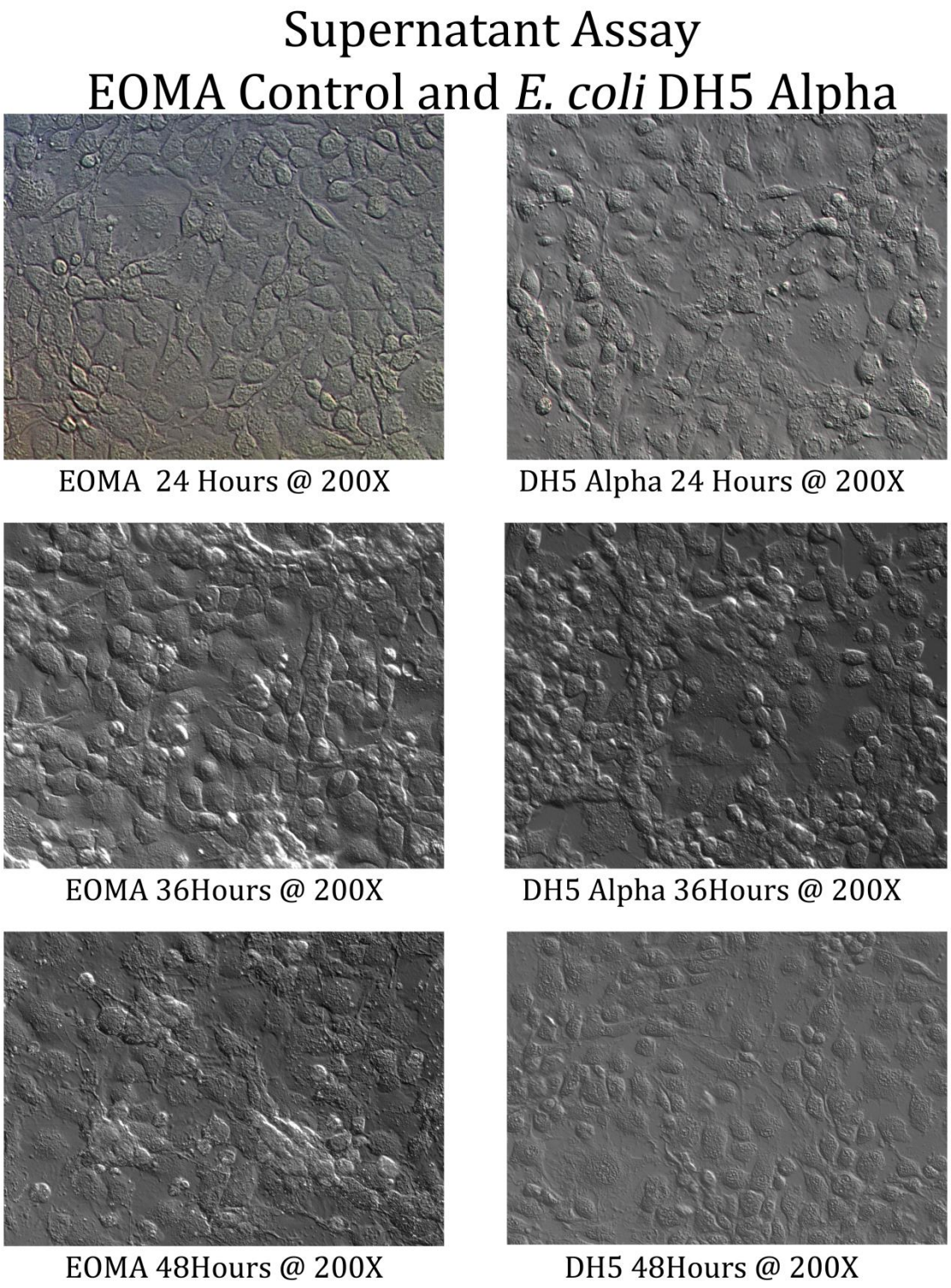

Figure 15: Supernatant Controls. The panel on the right shows EOMA supernatant-free control at 24, 36, and 48 hours at 200X magnification; the left panel shows DH5α supernatant at the same conditions.

Figure 16 shows the *C. sakazakii* BAA 894 supernatant assay on the right and the K1 *E. coli* control on the left at 200x magnification. At 24 hours, the K1 supernatant control shows a slight reduction in EOMA cell confluency with cells remaining overall confluent with normal morphology. In contrast, BAA 894 supernatant causes marked reduction in EOMA cell confluency at 24 hours. The monolayer appears slightly over 50% confluent with remaining cells showing more "stretched" cell shape than usual. At 36 hours, the K1 supernatant control begins to show a reduction in EOMA cell confluency and shows a change in cell morphology. The confluency remains above 75%, however the remaining attached EOMA cells begin to show rounding. Some detached dead cells can be seen. Before the image is captured from the live view, round (dead) cells are apparent from movement while attached cells remain fixed in view. At 36 hours, the BAA 894 supernatant shows reduced cell confluency below 25%. Remaining EOMA cells in the image are floating dead cells that have detached from the slide. Once the 48 hour time point is reached, more dead and floating cells can be seen with the K1 supernatant control. EOMA confluency is reduced to under 25% and few attached cells can be seen. BAA 894 supernatant shows nearly all EOMA cells to be dead and floating. Few remaining EOMA cells can be found attached to the slide at this time.

The supernatant assay shows time scale differences between the *E. coli* and *C. sakazakii* damage to EOMA cells as well illustrating cytotoxicity can be mediated by cell-free supernatant alone.

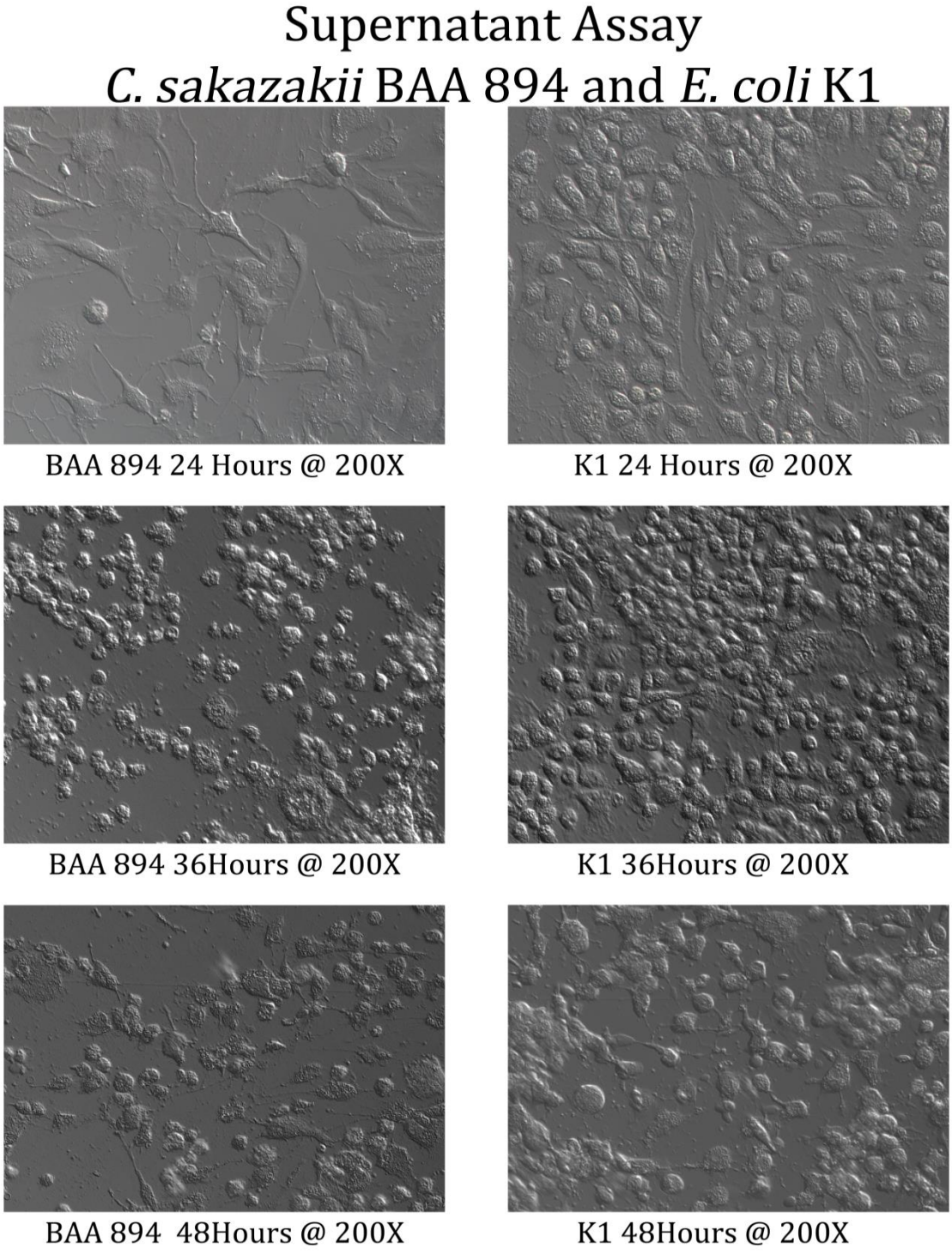

Figure 16: BAA 894 Supernatant Time Course. The panel on the right shows *C. sakazakii* BAA 894 supernatant at 24, 36, and 48 hours at 200X magnification; the right panel shows K1 supernatant at the same time points and magnification.

G**entamicin/ Adhesion Assays**

The Gentamicin and Adhesion Assays were performed to determine bacterial isolate ability to adhere to and invade EOMA cells as described by Berry et al (64). The original assay was designed to be used with uropathogenic *E. coli* and monolayers of mouse bladder cells (64). In addition to the *E. coli* controls and *C. sakazakii* isolates, *S. enterica* was used as an invasive control. When used with the EOMA cell line and *C. sakazakii* isolates, bacterial cells could not be detected at the endpoint of either the adhesion or gentamicin assay (data not shown).

Troubleshooting measures tested differented percentages of chemicals used and higher multiplicities of infection (MOI). It was determined that concentrations of chemicals used in the experiment were not affecting the bacterial cells. However, the multiplicity of infection and incubation times had marked effects on the ability to detect bacteria at experimental endpoints. The original protocol calls for a two hour incubation and MOI of 10. When given longer incubation times and higher MOI, endpoint bacterial cell counts could be detected (data not shown). An MOI of 10^2 or 10^3 is recommended with the use of all incubation times.

Due to time constraints and EOMA cell culture failure, these experiments with improved parameters were not able to be performed in triplicate. Therefore there is no data available for these procedures.

DISCUSSION

Experimental Model

Research in the Gibbs lab has focused on the development of an *in-vitro* system to study *C. sakazakii* invasion of the blood brain barrier through the use of an astrocyte and brain microvascular endothelial cell co-culture. This system utilizes trans endothelial electrical resistance (TEER) to measure the integrity of an intact barrier and to detect breeches in the barrier observed by reduced resistance. This system can be applied to identify isolates of bacterial species that are able to breech the barrier as well as aid in identifying the time course of barrier breech. Identification of crucial barrier time-points can be used to study: proteins expressed by bacteria at this time, gene expression levels, and may also be used to compare genotypes of virulent vs. non-virulent isolates within the species.

This MS thesis aimed to provide time-course image analysis of changes made to the first cells *C. sakazakii* would encounter *in vivo*, brain microvascular endothelial cells. In addition, known meningitis causing *C. sakazakii* isolates (BAA 894 and CT2) and fecal isolates (52 and N72 1A) were used to characterize phenotypic similarities and differences between isolates. All isolates showed similar growth rates, resistance to antibiotics, and showed great motility. The ability of individual isolates to damage monolayers of mouse endothelial cells (EOMA) varied by isolate and with incubation time. BAA 894 showed the greatest level of cell damage at rates that exceeded the *E. coli* K1 control, while other isolates required more time and caused less damage. In addition, EOMA cell damage was shown to occur independently of live *C. sakazakii* with the use of BAA 894. Adhesion and invasion of EOMA cells was not able to be determined using the existing protocol, but new parameters were investigated.

Blood Brain Barrier Invasion Requirements

In order for a pathogen to cause meningitis, it must first complete a number of steps including colonization of the tissue of entry, invasion of surrounding cells, survival and multiplication resulting in spread to the blood, and finally, entry into the brain by crossing the blood brain barrier (56, 57). Research suggests that *C. sakazakii* achieves these steps via an oral route through an initial contact with contaminated powdered infant formula followed by colonization and invasion of the gut epithelial cells leading to bacteremia (39, 59).

Once in the bloodstream, the bacteria not only survive but also maintain high levels before adherence to brain microvascular endothelial cells; Invasion of the barrier also requires cytoskeletal rearrangements and traversal as live bacteria (60). To mimic high rates of bacteremia, an inoculum of 10^8 bacterial cells/ml were used in cytotoxicity assays. Research revealed that 10^3 cfu/ml may be more appropriate as this is the level of bacteremia needed to cause meningitis in neonates (57). These assays showed that the mouse microvascular endothelial cells were unable to maintain cell confluency over time when co-cultured with *C. sakazakii* isolates (Figures 11-14). High levels of bacteria could affect confluency either by direct or indirect EOMA cell contact. Cytotoxicity assays showed that *C. sakazkii* isolates appear to cluster around cells and to fill the space between the cells. This could indicate that direct adhesion occurred; further studies of ligand-receptor interactions would elucidate the cell components involved.

In addition, the supernatant assays showed that live bacterial cells were not needed to cause EOMA cell damage and disruption of confluency (Figure 16). This indirect cause of damage is most likely due to LPS in combination with toxin(s).

Certain isolates of *Enterobacter*.(*Cronobacter* species) have been shown to adhere to brain microvascular endothelial cells (BMEC) in either diffuse or clustered patterns (51). In addition, isolates of *C. sakazakii* show isolate specific ability to invade BMECs at low, intermediate, and high levels (39). The new parameters for the Adhesion and Gentamicin assays will aid in determining two key points: 1) whether the isolates used are able to adhere and invade cells and 2) whether the mouse EOMA cell line is a suitable for use to represent blood brain barrier invasion in humans. If the EOMA cell line does not result in the same interactions seen in human brain microvascular endothelial cells, then an alternate cell line may be needed for more accurate representation.

Studies have also shown that *C. sakazakii* invasion of BMECs utilize signal transduction pathways associated with Akt/P13K pathway leading to cytoskeleton rearrangements (49, 50). Determining genetic differences between invasive versus non-invasive phenotypes of *C. sakazakii* may aid in identification of crucial factors necessary for invasion. These may include: ligand/receptor interactions or virulence factors that could induce such signaling. Utilizing stains specific for the cytoskeleton in conjunction with the current cytotoxicity assays could enable visualization of the process taking place.

Overall, the initial cytotoxicity and supernatant assays show that *C. sakazakii* isolates are able to grow in co-culture with the EOMA cell line and to cause substantial cell damage over time. The meningitis causing strains BAA 894 (Figure 11) and CT2 (Figure 13) showed considerable variation in their ability to cause damage to the cell monolayer. BAA 894 caused a substantial reduction in cell confluency within the first 24 hours of incubation; whereas; CT2 showed varying ability to damage the cell monolayer at all. These differences may be due to

differences between isolates or could indicate that the two isolates utilize different pathways to cross endothelial cells. It is interesting to note that the environmental isolates 52 (Figure 12) and N72 1A (Figure 14) both showed a consistent ability to damage EOMA cell confluency over the 24, 36, and 48 hour time points. These isolates have not been shown to cause meningitis, but through the use of the astrocyte-endothelial TEER system, may be shown to be pathogenic *in vitro*. Conversely, if these isolates are unable to penetrate the *in vitro* system, differences between meningitis and non-meningitis causing isolates may be elucidated.

Understanding differences and mechanistic pathways of invasion between pathogenic and non-pathogenic strains of bacteria could provide targets for novel treatment and prevention of infection.

BBB Pathogens

Pathogens may invade the blood-brain barrier in three different ways: transcellularly, paracellularly, or via survival in infected phagocytic cells (53, 60). Transcellular traversal of the blood brain barrier occurs when bacteria travel through an individual cell while paracellular transport involves movement between two adjacent cells (53).

C. sakazakii may be able to use multiple methods of traversal as suggested by its ability to invade both macrophages and brain microvascular endothelial cells (39, 45). Invasion of BMECs may indicate transcellular traversal while invasion of macrophages could support phagocytic transport. The present studies focus on investigating a transcellular mechanism in *C. sakazakii*. To investigate this pathway, EOMA cell invasion must be confirmed to ensure that the cell line is suitable for a human model. New parameters for use with the Invasion assay will be able to determine this ability in the future. Next, the molecular details of invasion and possible

cytoskeletal rearrangement can be characterized. In addition, further work with the cytoxicity and supernatant assays may aid in identifying key bacterial interactions or products necessary for live traversal of the blood brain barrier.

Meningitis causing pathogens of both prokaryote and eukaryote origin have been extensively reviewed and shown to use or are predicted to use one or a number of pathways as summarized in Table 4 below.

Table 4: Traversal of the Blood Brain Barrier

Organism	Domain	Mechanism of Traversal
Borrelia burgdorferia	Prokaryote	Paracellular (53, 60) Transcellular (54)
Trypanosoma species	Eukaryote	Paracellular (53, 54)
Listeria monocytogenes	Prokaryote	Phagocytic Transport as Live Bacteria (53, 54, 60) Transcellular (53, 54, 60)
Mycobacteria tuberculosis	Prokaryote	Phagocytic Transport as Live Bacteria (53, 54, 60) Transcellular (53, 54, 60)
Eschericia coli	Prokaryote	Transcellular (53, 54, 60)
Neisseria meningitidis	Prokaryote	Transcellular (53, 54, 60)
Group B Streptococci	Prokaryote	Transcellular (53, 54, 60)
Candida albicans	Eukaryote	Transcellular (53, 54, 60)

Mechanisms of Blood Brain Barrier Traversal by various meningitis causing prokaryotic and Eukaryotic organisms.

These pathogens are able to breach the BBB using various pathogen-specific host-microbe interactions including specific ligand-receptor interactions, activation of cytoskeleton signaling pathways, activation of host immune system and through the utilization of specific microbial proteins (53, 54, 56, 57).

As additional information on *C. sakazakii* is accumulated, comparison to other meningitis-causing pathogens may aid in identifying similar pathway sequences.

Escherichia coli K1 As A Model Organism

E. coli K1 is an encapsulated strain of *E. coli* that is able to survive in the blood, invade human brain microvascular endothelial cells (HBMEC), and can cause meningitis. It is often used as a model organism in both *in vitro* and *in vivo* meningitis studies (53, 57, 60) and served this purpose in this *in vitro* study. The transcellular invasion of *E. coli* K1 across the BBB has not been fully elucidated, although many bacterial components necessary for invasion have been discovered. After causing high levels of bacteremia in the blood, *E. coli* K1 must survive host immune defenses and both attach and invade HBMECs. K1 is able to survive in the blood due to the K1 antigen which provides serum resistance of bacterial killing (53, 57). To then attach to HBMECs, K1 utilizes Type 1 fimbrae, outer membrane protein OmpA, CNF1, and IbeB which provide adhesion and receptor-ligand attachment, and invasive ability (53, 57, 73–76). The bacterium then uses a transcellular "zipper" mechanism to trigger cytoskeletal rearrangements through the use of signal transduction pathways utilizing FAK, P13K, Src and Cpla2 (60, 73). Following cytoskeletal rearrangement, *E. coli* K1 survives in host vacuoles without replicating until crossing the barrier as live bacteria (57). These components have been compiled in Table 5 below.

Table 5 :*E. coli* K1 Requirements for BBB Invasion

Component	**Bacterial Function**	**Aid In BBB**
K1	Capsule	Serum Resistance (53, 57)
FimH	Adhesional Fimbraie	Binds HBMECs (53, 57)
OmpA	Outer membrane protein	Binds N-acetyl-glucosamine of HBMEC (53, 57, 73, 74)
IbeB	Invasion Locus	Aids in HBMEC invasion (53, 57, 74, 75)
Cytotoxic necrotizing factor 1 (CNF1)	Toxin	Aids in HBMEC Invasion (53, 57, 76)

E. coli K1 Components and their contributions to BBB invasion.

In an *in vitro* model, K1 strain RS218 does not disturb the HBMEC monolayer after 60 minute incubation, whereas in non-endothelial cell lines this strain causes cell rounding (77). The study utilized a monolayer of endothelial cells and TER with an MOI of 10 and showed that after the initial two hours of infection the monolayer retained cell morphology and initially increased electrical resistance (77).

The present investigation of mouse microvascular endothelial cells utilized time points beyond 2 hours to detail cell damage after 24, 36, and 48 hours of incubation. As detailed in cell control Figure 9, *E. coli* K1 begins to cause increasing damage and cell rounding to the monolayer of endothelial cells ending with a qualitative estimation of 75% loss in monolayer confluency after 48 hours. The DH5 α non-pathogenic control does not cause any apparent damage to endothelial cell monolayers at any time point. Previous studies from the Gibbs lab using the TEER co-culture of both endothelial cells and astrocytes indicate that the electrical resistance decreases over time after incubation with *E. coli* K1 (Welker and Gibbs, unpublished). Taken together with the cytoxicity assay showing increasing endothelial cell damage over time, these findings indicate that the endothelial barrier cannot sustain long-term exposure to this

organism. In terms of patient treatment, eliminating the infection after barrier traversal remains crucial to patient survival.

When researching *in vivo* models of *E. coli* K1 associated studies, RS218 was found to be used as a common control. Further investigation into the current K1 strain utilized for cell controls in the present assays revealed that the ATCC isolate 11775 is a BSL 1 organism and may not be associated with bacterial meningitis. This could mean that the results seen in these studies do not accurately reflect what is seen with a true meningitis causing K1 isolate. It is recommended that a proven meningitis-associated isolate such as RS218 be used as the positive meningitis causing control for future work with both monolayer and co-culture studies in the lab. This will ensure that the cytotoxic effects seen by the meningitis causing control are accurately represented.

C. sakazakii Characterization

The *C. sakazakii* isolates 52, BAA 894, CT2, and N72 1A were all shown to share similar physiological characteristics in terms of growth and antibiotic susceptibility as shown in Figure 2 and Table 3. Strains 52 and N72 1A were fecal isolates from bovine and bison respectively. BAA 894 is a meningitis-associated isolate obtained from the ATTC, while CT2 is also a meningitis-associated isolate from a clinical source. All *C. sakazakii* isolates appear to grow normally and at similar rates to the *E. coli* isolates used. With respect to the time course investigation, this excludes slower growth as reason for delayed damage during the time course investigation. Differences seen in cytotoxicity over time are a result of other differences between the bacteria. The antibiotic susceptibility patterns observed overall agree with what is found in the literature with respect to *C. sakazakii* sensitivities and resistance.

All isolates of *C. sakazakii* were also shown to be motile through the use of swarm plates (Figures 6 & 8) at both 25 and 37 ^{o}C. All isolates were shown to be more motile at 37^{o}C and BAA 894 showed the highest rates of motility at both temperatures. The significance of isolate motility is most likely important in food processing, and initial infection during necrotizing enterocolitis.

Cytotoxicity Variation

Cell cytotoxicity varied between isolates with BAA 894 showing earlier damage than other isolates and causing the greatest reduction in EOMA cell monolayer confluency. Surprisingly, the clinical meningitis-causing isolate CT2 showed varying ability to damage the EOMA cell monolayer between experimental trials. During some trials a high degree of damage was seen, while during experimental repeats at other times no damage was observed. This could be due to experimental error or could be due to variation in the isolate's ability to consistently express factors necessary for cell damage. Alternately, isolate CT2 may cause meningitis through survival in phagocytic cells, bypassing the need for direct barrier contact. BAA 894, 52, and N72 1A all showed increased damage to EOMA cell monolayers over time as shown in Figures 11-12 and 14. Figure 13 shows the variable ability of CT2 to damage the EOMA cell monolayer.

The mechanism that *C. sakazakii* uses to traverse the BBB is unknown. However, both transcellular and phagocytic traversal appear possible. *C. sakazakii* is able to invade HBMECs, possesses OmpA, and causes cytoskeletal rearrangement which would support transcellular traversal (53). Alternately, the organism's ability to survive within macrophages could facilitate penetration after surviving phagocytosis (53). As shown in Table 4, some pathogens utilize more than one pathway to cross the BBB therefore *C. sakazakiii* could do the same.

Two methods of transcellular BBB penetration are possible using either the "zipper" or "trigger" mechanism; The zipper mechanism requires direct cell contact while the trigger mechanism acts through indirect contact (60). As described above, *E. coli* K1 utilizes OmpA for direct HBMEC contact. Studies have shown *C. sakazakii* requires OmpA and OmpX for invasion of intestinal epithelial cells which supports the use of the zipper mechanism (40).Invasion of endothelial cells has also been shown to be dependent on these OmpA, although it's interaction with HBMECs receptors may differ from that of K1 (78). Different mechanisms could be used by *C. sakazakii* for different cell types. Staining the cytoskeleton in conjunction with this assay may show whether direct bacterial contact occurs which would support the zipper mechanism. These images would show whether direct contact or "ruffling" occurs.

Supernatant Cytotoxicity Investigation

To begin to investigate an indirect mechanism and to further detail monolayer damage, cell-free supernatant cytotoxicity assays were performed. As the only consistently cytotoxic meningitis-causing isolate, BAA 894 was chosen for further use. Confluent monolayers of EOMA cells were inoculated with cell-free BAA 894 supernatant from an overnight culture. Figure 16 details the early damage caused to the monolayer at 24 hours and near-complete destruction of the monolayer after 48 ours. These findings suggest toxin-mediated damage to the EOMA cell lines. This damage could be a result of a single toxin or multiple toxins acting together. Separating supernatant components by cell fraction via high performance liquid chromatography would aid in isolation of the damaging toxin(s). Toxin-mediated entry into EOMA cells would support the trigger mechanism of entry.

Significance to Society

Bacterial meningitis causes approximately 1.2 million cases/year worldwide and contributed to approximately 393,000 deaths in neonates in 2010 (79, 80). Newborns and children are at higher risk for bacterial meningitis as well as those in developing nations or with compromised immune systems (80). While *C. sakazakii's* contributions to these rates may be small, it has been recognized as an emerging pathogen (28, 59). Understanding the mechanisms of blood brain barrier traversal in *C. sakazakii* may contribute to existing knowledge of bacterial mechanisms which may in turn contribute to prevention, control, and treatment measures. Investigating the main cell lines involved in the BBB will establish the groundwork for this understanding.

The link between contaminated infant formula and *C. sakazakii* associated neonatal meningitis underscores the need for understanding disease development in infants. The blood brain barrier develops from the neonatal to adult stages resulting in a progressive tightening of the barrier (52). Identifying the components of the BBB targeted by these bacterial cells will enhance our understanding of the disease mechanism and will allow for comparison between neonatal and adult barriers. Identifying whether key features make neonates more susceptible to invasion will provide a target for prevention and treatment.

Further, development of an *in vitro* mouse system for the study of the major cell lines involved in BBB formation may be widely used with other species. As the molecular details of bacterial traversal are elucidated, bacterial isolates can be studied with respect to their ability to cause the same damage in knockouts. Additionally, in a meningitis outbreak situation, suspected environmental isolates could be screened using the system to assess the potential to damage brain

microvascular endothelial cells and astrocytes. If reliable, such an assessment would contribute to the identification of the causative agent of disease.

Future Work

Several future studies could expand upon the work presented in this thesis including: identifying receptors involved in bacterial adhesion, further investigation into the possibility of toxin mediated damage, and biofilm investigation.

Utilizing a higher MOI (10^2-10^3) with the Gentamicin/Adhesion assay will show the degree of bacterial adhesion to EOMA cells as well as whether *C. sakazakii* is able to invade the mouse cell line. This will allow for invasion rates to be characterized among meningitis and fecal isolates. The adhesion portion of the assay could potentially be used for determining ligand-receptor interactions and could be used to identify genes necessary for adhesion (in addition to OmpA). A library of mutated *C. sakazakii* BAA 894 could be constructed and then subjected to the adhesion assay. Mutants unable to adhere to EOMA cells could then be further studied for a genetic basis for differences seen between mutants and the wild type. Sequencing non-adherent mutants will help identify the sequences that are missing/altered. Once these regions are known, the intact gene(s) from the wild type could be isolated and cloned into a plasmid/reporter system and transformed back into the original mutant. Regaining the ability to adhere to cells will confirm the necessity for attachment. In addition, if the reporter system is fluorescently labeled, localized adhesion with EOMA cells could be identified and suspected receptors could be investigated. Receptors that are believed to be necessary for attachment could be blocked by antibodies tagged in an alternate fluorescent color. Maintained fluorescence associated with the mutated bacteria would indicate the correct receptor was not blocked while a lack of

fluorescence by the bacteria would confirm it is. Using the alternate fluorescent tag would confirm antibody attachment.

The supernatant assay could be used to study the possibility of toxin mediated damage in a number of ways. First, the supernatant could be heated before incubation to determine if heat labile toxins are present. An inability to cause the same damage would indicate the proteins were denatured while no change cytotoxicity would indicate heat stabile toxins or other factors present in the supernatant. If heat stabile toxins are present, the supernatant could be fractioned into separate components using high performance liquid chromatography. Once separated individual components could be incubated alone and in combination to determine which portion(s) are necessary for damage. In addition, the concentration necessary for damage could be determined using a serial dilution of the necessary component(s). If a portion of the supernatant is necessary to cause damage it could be identified multiple ways. Again a mutant library could be constructed to determine a possible genetic component. Alternately further purification of the component could be used to determine protein structure utilizing either crystallography or NMR.

Researching the role of *C. sakazakii* motility in the contribution to biofilm formation could provide targets for prevention on manufacturing surfaces in the food industry. The ability to form biofilms on stainless steel could cause contamination in factories that produce either powdered infant formula or follow up formula. Preventing these biofilms from forming would help eliminate this route of contamination. The Pruess lab has investigated chemicals that inhibit or reduce biofilm formation in *E. coli*. These same chemicals could be screened with *C. sakazakii* to determine which may be suitable for use and whether they are effective with stainless steel.

A collaboration with an engineering group could also be used to develop a novel microscopy system to study the time course of *C. sakazakii* penetration of both the astrocytes and EOMA cells. Combining the ideas of the TEER system and a simple flow cell, an advance type of flow cell could be created. This cell would allow for two cells lines to grow on opposites sides of a mesh surface that lies between two viewing surfaces. The device would allow for microscopy of both cell lines and would incorporate separate media lines for the divided sides of the device. The rate of media flow could be calibrated to mimic the rate of blood flow to the brain.

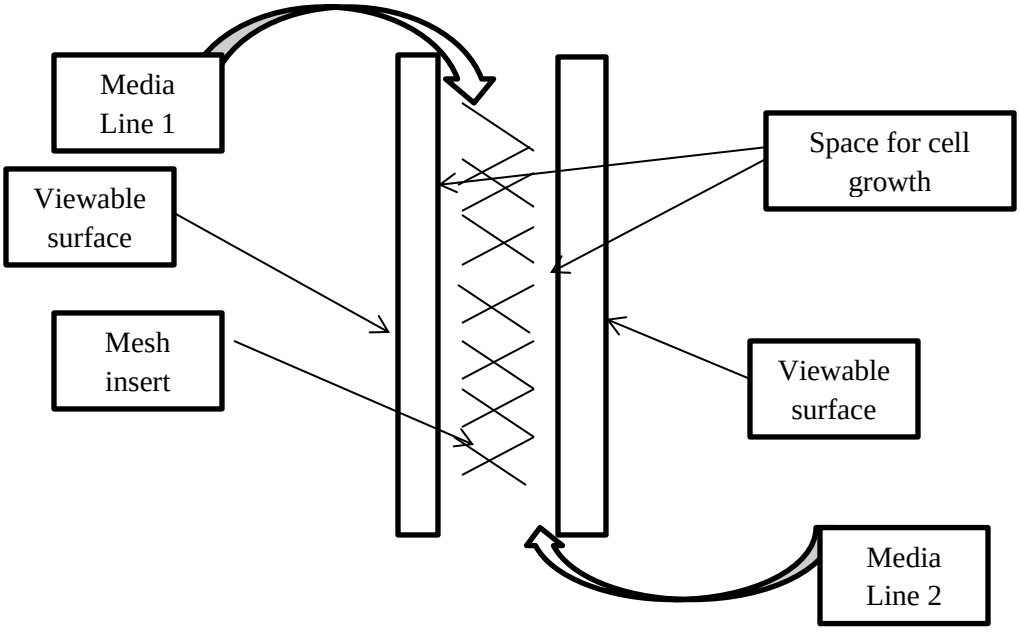

Figure 17: Proposed Design for the Advanced Flow Cell.

Experimentation could proceed as follows. Astrocytes and endothelial cells would be grown on the mesh surface similar to how a TEER insert is used. Confluency of both cell lines could be ensured by viewing either side of the device with a microscope. Once confluent, the media line to the side of the device containing EOMA cells would be inoculated with bacteria at rates known to cause meningitis in infants. If the bacteria are able to cross both cell lines, the

sterile media line for the astrocyte side of the cell would become contaminated. Images could be taken at any point of the experiment to determine how the cells are affected. These images would show what the TEER system of cells look like at similar time points. It would also show whether confluency of either cell line is reduced.

The TEER and advanced flow cell device could be provide even further insight into *C. sakazakii* interactions with the incorporation of other BBB cells such as pericytes and microglial cells which could be layered with the EOMA and astrocytes respectively. A number of advanced imaging techniques could be used to determine interactions at various locations and between all cell types. Utilizing these cell lines would more accurately reflect true blood brain barrier traversal and could be used to study bacterial mutants, cell receptor interactions and other pathogens as described previously.

REFERENCES

1. 2012. CDC Features: Cronobacter Illness and Infant Formula. Centers For Disease Control and prevention.
2. **Farmer, J.J. III, Davis,Betty R, Hickman-Brenner,F.W., McWhorter,Alma, Huntley-Carter,G.P., Asbury,M.A., Riddle,Conradine, Wathen-Grady,H.G., Elias,C., Fanning,G.R., Steigerwalt,A.G, O'Hara,Caroline M., Morris,G.K., Smith,P.B., Brenner,Don J.** 1985. Biochemical Identification of New Species and Biogroups of Enterobacteriaceae Isolated from Clinical Specimens. J. Clin. Microbiol. **21**:46–76.
3. **Farmer JJ, Asbury MA, Hickman FW, Brenner DJ, THE ENTEROBACTERIACEAE STUDY GROUP**. 1980. Enterobacter sakazakii: A New Species of "Enterobacteriaceae" Isolated from Clinical Specimens. Int. J. Syst. Bacteriol. **30**:569–584.
4. **Iversen C, Lehner A, Mullane N, Bidlas E, Cleenwerck I, Marugg J, Fanning S, Stephan R, Joosten H**. 2007. The taxonomy of Enterobacter sakazakii: proposal of a new genus Cronobacter gen. nov. and descriptions of Cronobacter sakazakii comb. nov. Cronobacter sakazakii subsp. sakazakii, comb. nov., Cronobacter sakazakii subsp. malonaticus subsp. nov., Cronobacter turicensis sp. nov., Cronobacter muytjensii sp. nov., Cronobacter dublinensis sp. nov. and Cronobacter genomospecies 1. BMC Evol. Biol. **7**:64.
5. **Iversen C, Lehner A, Mullane N, Marugg J, Fanning S, Stephan R, Joosten H**. 2007. Identification of "Cronobacter" spp. (Enterobacter sakazakii). J. Clin. Microbiol. **45**:3814–3816.
6. **Brady C, Cleenwerck I, Venter S, Coutinho T, De Vos P**. 2013. Taxonomic evaluation of the genus Enterobacter based on multilocus sequence analysis (MLSA): Proposal to reclassify E. nimipressuralis and E. amnigenus into Lelliottia gen. nov. as Lelliottia nimipressuralis comb. nov. and Lelliottia amnigena comb. nov., respectively, E. gergoviae and E. pyrinus into Pluralibacter gen. nov. as Pluralibacter gergoviae comb. nov. and Pluralibacter pyrinus comb. nov., respectively, E. cowanii, E. radicincitans, E. oryzae and E. arachidis into Kosakonia gen. nov. as Kosakonia cowanii comb. nov., Kosakonia radicincitans comb. nov., Kosakonia oryzae comb. nov. and Kosakonia arachidis comb. nov., respectively, and E. turicensis, E. helveticus and E. pulveris into Cronobacter as Cronobacter zurichensis nom. nov., Cronobacter helveticus comb. nov. and Cronobacter pulveris comb. nov., respectively, and emended description of the genera Enterobacter and Cronobacter. Syst. Appl. Microbiol. **36**:309–319.
7. **Joseph S, Cetinkaya E, Drahovska H, Levican A, Figueras MJ, Forsythe SJ**. 2011. Cronobacter condimenti sp. nov., isolated from spiced meat, and Cronobacter universalis sp. nov., a species designation for Cronobacter sp. genomospecies 1, recovered from a leg infection, water and food ingredients. Int. J. Syst. Evol. Microbiol. **62**:1277–1283.
8. **Masood N, Moore K, Farbos A, Hariri S, Paszkiewicz K, Dickins B, McNally A, Forsythe S**. 2013. Draft Genome Sequences of Three Newly Identified Species in the Genus Cronobacter, C. helveticus LMG23732T, C. pulveris LMG24059, and C. zurichensis LMG23730T. Genome Announc. **1**:e00783–13–e00783–13.
9. **Stephan R, Van Trappen S, Cleenwerck I, Iversen C, Joosten H, De Vos P, Lehner A**. 2008. Enterobacter pulveris sp. nov., isolated from fruit powder, infant formula and an infant formula production environment. Int. J. Syst. Evol. Microbiol. **58**:237–241.

10. **Stephan R, Van Trappen S, Cleenwerck I, Vancanneyt M, De Vos P, Lehner A**. 2007. Enterobacter turicensis sp. nov. and Enterobacter helveticus sp. nov., isolated from fruit powder. Int. J. Syst. Evol. Microbiol. **57**:820–826.
11. **Kosako Y**. 2002. Riichi Sakazaki 1920--2002. Int. J. Syst. Evol. Microbiol. **52**:1435–1435.
12. **Graves R**. 2012. The Greek myths. Penguin Books, New York.
13. **Day M**. 2007. Barron's 100 characters from classical mythology: discover the fascinating stories of the Greek and Roman deities1st ed. for North America. Barron's Educational Series, Inc, Hauppauge, NY.
14. **Marieb, Elaine N. , R.N., Ph.D**. 2004. Human Anatomy & Physiology, 6th ed. Daryl Fox, San Francisco, CA.
15. **Joseph S, Sonbol H, Hariri S, Desai P, McClelland M, Forsythe SJ**. 2012. Diversity of the Cronobacter Genus as Revealed by Multilocus Sequence Typing. J. Clin. Microbiol. **50**:3031–3039.
16. **Joseph S, Desai P, Ji Y, Cummings CA, Shih R, Degoricija L, Rico A, Brzoska P, Hamby SE, Masood N, Hariri S, Sonbol H, Chuzhanova N, McClelland M, Furtado MR, Forsythe SJ**. 2012. Comparative Analysis of Genome Sequences Covering the Seven Cronobacter Species. PLoS ONE **7**:e49455.
17. **Iversen C, Lane M, Forsythe SJ**. 2004. The growth profile, thermotolerance and biofilm formation of Enterobacter sakazakii grown in infant formula milk. Lett. Appl. Microbiol. **38**:378–382.
18. **Breeuwer P, Lardeau A, Peterz M, Joosten HM**. 2003. Desiccation and heat tolerance of Enterobacter sakazakii. J. Appl. Microbiol. **95**:967–973.
19. **Al-Nabulsi AA, Osaili TM, Elabedeen NAZ, Jaradat ZW, Shaker RR, Kheirallah KA, Tarazi YH, Holley RA**. 2011. Impact of environmental stress desiccation, acidity, alkalinity, heat or cold on antibiotic susceptibility of Cronobacter sakazakii. Int. J. Food Microbiol. **146**:137–143.
20. **Arroyo C, Condón S, Pagán R**. 2009. Thermobacteriological characterization of Enterobacter sakazakii. Int. J. Food Microbiol. **136**:110–118.
21. **Shaker RR, Osaili TM, Abu Al-Hasan AS, Ayyash MM, Forsythe SJ**. 2008. Effect of desiccation, starvation, heat, and cold stresses on the thermal resistance of Enterobacter sakazakii in rehydrated infant milk formula. J. Food Sci. **73**:M354–359.
22. **Friedemann M**. 2007. Enterobacter sakazakii in food and beverages (other than infant formula and milk powder). Int. J. Food Microbiol. **116**:1–10.
23. **Kandhai MC, Reij MW, Gorris LGM, Guillaume-Gentil O, van Schothorst M**. 2004. Occurrence of Enterobacter sakazakii in food production environments and households. Lancet **363**:39–40.
24. **Muytjens HL, Roelofs-Willemse H, Jaspar GH**. 1988. Quality of powdered substitutes for breast milk with regard to members of the family Enterobacteriaceae. J. Clin. Microbiol. **26**:743–746.
25. **Butler JF, Garcia-Maruniak A, Meek F, Maruniak JE**. 2010. Wild Florida House Flies (*Musca domestica*) as Carriers of Pathogenic Bacteria. Fla. Entomol. **93**:218–223.
26. **Schmid M, Iversen C, Gontia I, Stephan R, Hofmann A, Hartmann A, Jha B, Eberl L, Riedel K, Lehner A**. 2009. Evidence for a plant-associated natural habitat for Cronobacter spp. Res. Microbiol. **160**:608–614.

27. **Biering G, Karlsson S, Clark NC, Jónsdóttir KE, Lúdvígsson P, Steingrímsson O**. 1989. Three cases of neonatal meningitis caused by Enterobacter sakazakii in powdered milk. J. Clin. Microbiol. **27**:2054–2056.
28. **FAO/WHO**. 2008. Enterobacter sakazakii (Cronobacter spp.) in powdered follow-up formulae. 15. Meeting Report, Food and Agriculture Organization of the United Nations & World Health Organization, Rome.
29. **Block C, Peleg O, Minster N, Bar-Oz B, Simhon A, Arad I, Shapiro M**. 2002. Cluster of neonatal infections in Jerusalem due to unusual biochemical variant of Enterobacter sakazakii. Eur. J. Clin. Microbiol. Infect. Dis. Off. Publ. Eur. Soc. Clin. Microbiol. **21**:613–616.
30. **Muytjens HL, Zanen HC, Sonderkamp HJ, Kollée LA, Wachsmuth IK, Farmer JJ 3rd**. 1983. Analysis of eight cases of neonatal meningitis and sepsis due to Enterobacter sakazakii. J. Clin. Microbiol. **18**:115–120.
31. **Simmons BP, Gelfand MS, Haas M, Metts L, Ferguson J**. 1989. Enterobacter sakazakii infections in neonates associated with intrinsic contamination of a powdered infant formula. Infect. Control Hosp. Epidemiol. Off. J. Soc. Hosp. Epidemiol. Am. **10**:398–401.
32. **Lai KK**. 2001. Enterobacter sakazakii infections among neonates, infants, children, and adults. Case reports and a review of the literature. Medicine (Baltimore) **80**:113–122.
33. **Barron JC, Forsythe SJ**. 2007. Dry stress and survival time of Enterobacter sakazakii and other Enterobacteriaceae in dehydrated powdered infant formula. J. Food Prot. **70**:2111–2117.
34. **Nazarowec-White M, Farber JM**. 1997. Thermal resistance of Enterobacter sakazakii in reconstituted dried-infant formula. Lett. Appl. Microbiol. **24**:9–13.
35. **Williams TL, Monday SR, Edelson-Mammel S, Buchanan R, Musser SM**. 2005. A top-down proteomics approach for differentiating thermal resistant strains of Enterobacter sakazakii. Proteomics **5**:4161–4169.
36. **Gajdosova J, Benedikovicova K, Kamodyova N, Tothova L, Kaclikova E, Stuchlik S, Turna J, Drahovska H**. 2011. Analysis of the DNA region mediating increased thermotolerance at 58°C in Cronobacter sp. and other enterobacterial strains. Antonie Van Leeuwenhoek **100**:279–289.
37. **Townsend S, Hurrell E, Forsythe S**. 2008. Virulence studies of Enterobacter sakazakii isolates associated with a neonatal intensive care unit outbreak. BMC Microbiol. **8**:64.
38. **Joseph S, Forsythe SJ**. 2011. Predominance of Cronobacter sakazakii sequence type 4 in neonatal infections. Emerg. Infect. Dis. **17**:1713–1715.
39. **Giri CP, Shima K, Tall BD, Curtis S, Sathyamoorthy V, Hanisch B, Kim KS, Kopecko DJ**. 2012. Cronobacter spp. (previously Enterobacter sakazakii) invade and translocate across both cultured human intestinal epithelial cells and human brain microvascular endothelial cells. Microb. Pathog. **52**:140–147.
40. **Kim K, Kim K-P, Choi J, Lim J-A, Lee J, Hwang S, Ryu S**. 2010. Outer Membrane Proteins A (OmpA) and X (OmpX) Are Essential for Basolateral Invasion of Cronobacter sakazakii. Appl. Environ. Microbiol. **76**:5188–5198.
41. **Franco AA, Kothary MH, Gopinath G, Jarvis KG, Grim CJ, Hu L, Datta AR, McCardell BA, Tall BD**. 2011. Cpa, the outer membrane protease of Cronobacter sakazakii, activates plasminogen and mediates resistance to serum bactericidal activity. Infect. Immun. **79**:1578–1587.
42. **Centers For Disease Control and Prevention**. 2012. Bacterial Meningitis.

43. **Kim H, Ryu J-H, Beuchat LR**. 2006. Attachment of and biofilm formation by Enterobacter sakazakii on stainless steel and enteral feeding tubes. Appl. Environ. Microbiol. **72**:5846–5856.
44. **Franco AA, Hu L, Grim CJ, Gopinath G, Sathyamoorthy V, Jarvis KG, Lee C, Sadowski J, Kim J, Kothary MH, McCardell BA, Tall BD**. 2011. Characterization of putative virulence genes on the related RepFIB plasmids harbored by Cronobacter spp. Appl. Environ. Microbiol. **77**:3255–3267.
45. **Townsend SM, Hurrell E, Gonzalez-Gomez I, Lowe J, Frye JG, Forsythe S, Badger JL**. 2007. Enterobacter sakazakii invades brain capillary endothelial cells, persists in human macrophages influencing cytokine secretion and induces severe brain pathology in the neonatal rat. Microbiol. Read. Engl. **153**:3538–3547.
46. **Kothary MH, McCardell BA, Frazar CD, Deer D, Tall BD**. 2007. Characterization of the zinc-containing metalloprotease encoded by zpx and development of a species-specific detection method for Enterobacter sakazakii. Appl. Environ. Microbiol. **73**:4142–4151.
47. **Townsend S, Caubilla Barron J, Loc-Carrillo C, Forsythe S**. 2007. The presence of endotoxin in powdered infant formula milk and the influence of endotoxin and Enterobacter sakazakii on bacterial translocation in the infant rat. Food Microbiol. **24**:67–74.
48. **Kim K-P, Loessner MJ**. 2008. Enterobacter sakazakii invasion in human intestinal Caco-2 cells requires the host cell cytoskeleton and is enhanced by disruption of tight junction. Infect. Immun. **76**:562–570.
49. **Liu D-X, Zhao W-D, Fang W-G, Chen Y-H**. 2012. cPLA2α-mediated actin rearrangements downstream of the Akt signaling is required for Cronobacter sakazakii invasion into brain endothelial cells. Biochem. Biophys. Res. Commun. **417**:925–930.
50. **Li Q, Zhao W-D, Zhang K, Fang W-G, Hu Y, Wu S-H, Chen Y-H**. 2010. PI3K-dependent host cell actin rearrangements are required for Cronobacter sakazakii invasion of human brain microvascular endothelial cells. Med. Microbiol. Immunol. (Berl.) **199**:333–340.
51. **Jean-Philippe Mange, Roger Stephan, Nicole Borel, Peter Wild, Kwang Sik Kim, Andreas Pospischil, Angelika Lehner**. 2006. Adhesive properties of Enterobacter sakazakii to human epithelial and brain microvascular endothelial cells. BMC Microbiol. **6**.
52. **Abbott NJ**. 2002. Astrocyte-endothelial interactions and blood-brain barrier permeability. J. Anat. **200**:629–638.
53. **Kim KS**. 2008. Mechanisms of microbial traversal of the blood-brain barrier. Nat. Rev. Microbiol. **6**:625–634.
54. **Pulzova L, Bhide MR, Andrej K**. 2009. Pathogen translocation across the blood-brain barrier. FEMS Immunol. Med. Microbiol. **57**:203–213.
55. **Wolburg H, Lippoldt A**. 2002. Tight junctions of the blood-brain barrier: development, composition and regulation. Vascul. Pharmacol. **38**:323–337.
56. **Scheld WM, Koedel U, Nathan B, Pfister H-W**. 2002. Pathophysiology of bacterial meningitis: mechanism(s) of neuronal injury. J. Infect. Dis. **186 Suppl 2**:S225–233.
57. **Kim KS**. 2003. Pathogenesis of bacterial meningitis: from bacteraemia to neuronal injury. Nat. Rev. Neurosci. **4**:376–385.
58. **Kim KS**. 2003. Neurological diseases: Pathogenesis of bacterial meningitis: from bacteraemia to neuronal injury. Nat. Rev. Neurosci. **4**:376–385.
59. **American Society for Microbiology**. 2008. Enterobacter sakazakii. ASM Press, Washington, D.C.

60. **Kim KS**. 2006. Microbial translocation of the blood-brain barrier. Int. J. Parasitol. **36**:607–614.
61. **Neidhardt FC, Ingraham JL, Schaechter M**. 1990. Physiology of the bacterial cell: a molecular approach. Sinauer Associates, Sunderland.
62. **Wolfe, A J, Berg, H C**. 1989. Migration of bacteria in semisolid agar, p. 69736977. *In* Proceedings of the National Academy of Sciences in the United States of America.
63. 2007. BD BBL Sensi-Disc Antimicrobial Susceptibility Test Discs. Beckton, Dickinson Company.
64. **Berry RE, Klumpp DJ, Schaeffer AJ**. 2009. Urothelial cultures support intracellular bacterial community formation by uropathogenic Escherichia coli. Infect. Immun. **77**:2762–2772.
65. **Todar, K**. Todar's Online Textbook of Bacteriology. Madison, WI.
66. 1997. Escherichia coli K-12 Derivatives Final Risk Assessment. Final Risk Assessment, Environmental Protection Agency.
67. **Chart H, Smith HR, La Ragione RM, Woodward MJ**. 2000. An investigation into the pathogenic properties of Escherichia coli strains BLR, BL21, DH5alpha and EQ1. J. Appl. Microbiol. **89**:1048–1058.
68. **Paisley JW, Washington JA 2nd**. 1979. Susceptibility of Escherichia coli K1 to four combinations of antimicrobial agents potentially useful for treatment of neonatal meningitis. J. Infect. Dis. **140**:183–191.
69. **Larry Maturin, James T. Peeler**. 2001. Bacteriological Analytical Manual (BAM).
70. **McClave JT, Sincich T**. 2009. Statistics. Pearson Prentice Hall, Upper Saddle River, N.J.
71. **Centers for Disease Control and Prevention (CDC)**. 2002. Enterobacter sakazakii infections associated with the use of powdered infant formula--Tennessee, 2001. MMWR Morb. Mortal. Wkly. Rep. **51**:297–300.
72. **Kucerova E, Clifton SW, Xia X-Q, Long F, Porwollik S, Fulton L, Fronick C, Minx P, Kyung K, Warren W, Fulton R, Feng D, Wollam A, Shah N, Bhonagiri V, Nash WE, Hallsworth-Pepin K, Wilson RK, McClelland M, Forsythe SJ**. 2010. Genome Sequence of Cronobacter sakazakii BAA-894 and Comparative Genomic Hybridization Analysis with Other Cronobacter Species. PLoS ONE **5**:e9556.
73. **Kim KS**. 2002. Strategy of Escherichia coli for crossing the blood-brain barrier. J. Infect. Dis. **186 Suppl 2**:S220–224.
74. **Wang Y, Kim KS**. 2002. Role of OmpA and IbeB in Escherichia coli K1 invasion of brain microvascular endothelial cells in vitro and in vivo. Pediatr. Res. **51**:559–563.
75. **Huang SH, Chen YH, Fu Q, Stins M, Wang Y, Wass C, Kim KS**. 1999. Identification and characterization of an Escherichia coli invasion gene locus, ibeB, required for penetration of brain microvascular endothelial cells. Infect. Immun. **67**:2103–2109.
76. **Boquet P**. 2001. The cytotoxic necrotizing factor 1 (CNF1) from Escherichia coli. Toxicon Off. J. Int. Soc. Toxinology **39**:1673–1680.
77. **Paul-Satyaseela M, Xie Y, Di Cello F, Kim KS**. 2006. Responses of brain and non-brain endothelial cells to meningitis-causing Escherichia coli K1. Biochem. Biophys. Res. Commun. **342**:81–85.
78. **Singamsetty VK, Wang Y, Shimada H, Prasadarao NV**. 2008. Outer membrane protein A expression in Enterobacter sakazakii is required to induce microtubule condensation in human brain microvascular endothelial cells for invasion. Microb. Pathog. **45**:181–191.

79. **Liu L, Johnson HL, Cousens S, Perin J, Scott S, Lawn JE, Rudan I, Campbell H, Cibulskis R, Li M, Mathers C, Black RE, Child Health Epidemiology Reference Group of WHO and UNICEF**. 2012. Global, regional, and national causes of child mortality: an updated systematic analysis for 2010 with time trends since 2000. Lancet **379**:2151–2161.
80. **Castillo, Dana, Harcourt, Brian, Hatcher, Cynthia, Jackson, Michael, Katz, Lee, Mair, Raydel, Mayer, Leonard, Novak, Ryan, Rahalison, Lila, Schmink, Susanna, Theodore, M., Thomas, Jennifer, Vuong, Jeni, Wang, Xin**. 2011. Laboratory Methods for the Diagnosis of Meningitis caused by Neisseria meningitidi , Streptococcus pneumoniae, and Haemophilus influenzae, 2nd ed.